

## Coastal Sea Level and Related Fields from Existing Observing Systems

Marcos Marta <sup>1,2,\*</sup>, Wöppelmann Guy <sup>3</sup>, Matthews Andrew <sup>4</sup>, Ponte Rui M. <sup>5</sup>, Birol Florence <sup>6</sup>, Arduin Fabrice <sup>7</sup>, Coco Giovanni <sup>8</sup>, Santamaría-Gómez Alvaro <sup>9</sup>, Ballu Valerie <sup>3</sup>, Testut Laurent <sup>3</sup>, Chambers Don <sup>10</sup>, Stopa Justin <sup>11</sup>

<sup>1</sup> IMEDEA(UIB-CSIC), Miquel Marquès, 21, 07190 Esporles, Spain

<sup>2</sup> Department of Physics, University of the Balearic Islands, Cra. Valldemossa, km 7.5, 07122 Palma, Spain

<sup>3</sup> LIENSs, Université de La Rochelle, 2 Rue Olympe de Gouges, 17000 La Rochelle, France

<sup>4</sup> National Oceanography Centre, Joseph Proudman Building, 6 Brownlow Street, Liverpool L3 5DA, UK

<sup>5</sup> Atmospheric and Environmental Research, Inc., 131 Hartwell Avenue, Lexington, MA 02421, USA

<sup>6</sup> LEGOS, University of Toulouse, IRD, CNES, CNRS, 14 Avenue Edouard Belin, 31400 Toulouse, France

<sup>7</sup> CNRS, IRD, Ifremer, Laboratoire d'Océanographie Physique et Spatiale (LOPS), IUEM, Univ. Brest, 1625 Route de Sainte-Anne, 29280 Plouzané, France

<sup>8</sup> Faculty of Science, School of Environment, University of Auckland, Building 302, 23 Symonds Street, Private Bag 92019, Auckland 1142, New Zealand

<sup>9</sup> GET, Observatoire Midi-Pyrénées, CNRS, IRD, UPS, Université de Toulouse, 14 avenue Edouard Belin, 31400 Toulouse, France

<sup>10</sup> College of Marine Science, University of South Florida, 140 7th Ave S, MSL119, St. Petersburg, FL 33701.5016, USA

<sup>11</sup> University of Hawaii, 2540 Dole Street, Holmes Hall 405, Honolulu, HI 96822, USA

\* Corresponding author : Marta Marcos, email address : [marta.marcos@uib.es](mailto:marta.marcos@uib.es)

### Abstract :

We review the status of current sea-level observing systems with a focus on the coastal zone. Tide gauges are the major source of coastal sea-level observations monitoring most of the world coastlines, although with limited extent in Africa and part of South America. The longest tide gauge records, however, are unevenly distributed and mostly concentrated along the European and North American coasts. Tide gauges measure relative sea level but the monitoring of vertical land motion through high-precision GNSS, despite being essential to disentangle land and ocean contributions in tide gauge records, is only available in a limited number of stations. (25% of tide gauges have a GNSS station at less than 10 km.) Other data sources are new in situ observing systems fostered by recent progress in GNSS data processing (e.g., GPS reflectometry, GNSS-towed platforms) and coastal altimetry currently measuring sea level as close as 5 km from the coastline. Understanding observed coastal sea level also requires information on various contributing processes, and we provide an overview of some other relevant observing systems, including those on (offshore and coastal) wind waves and water density and mass changes.

---

**Keywords** : Sea-level observations, Tide gauges, Coastal altimetry, GNSS, Wind waves, Ocean bottom pressure, Hydrography

41

## 42 **1. Introduction**

43 Measurements of sea level at the coast have long been required for several purposes, such as  
44 for the definition of a reference level for national height systems (e.g. Woppelmann et al., 2014)  
45 or for harbour operations and navigation, besides the scientific motivation to understand the  
46 changes in sea level and their forcing mechanisms. Coastal sea-level monitoring is nowadays  
47 becoming increasingly important as it is a key component of operational oceanographic  
48 services aimed at ensuring harbour operability and safety and at generating accurate hazard  
49 forecasting and reliable flood or tsunami warning systems. With sea level rise in response to  
50 anthropogenic global warming being one of the major threats to the coastal zones, sea-level  
51 observations are also essential to quantify the coastal response to the different forcings and thus  
52 to determine the potential impacts of future sea-level rise on coastal populations, ecosystems  
53 and assets.

54 Coastal sea level is driven by several physical processes acting at many time scales, from  
55 seconds (including the effect of wind-waves) to millennia (for a review of the most relevant  
56 processes see Woodworth et al., this issue). Understanding this wide range of variability in sea  
57 level, therefore, requires considerable information, not only on the amplitude and frequency of  
58 coastal sea-level variations, but also on the characteristics of the individual contributors as well  
59 as on their possible interactions. In this sense, coastal sea-level observations can be seen as one  
60 component of a multi-platform observing system aimed at accurately monitoring the physical  
61 processes taking place in the oceans.

62 Observing systems for coastal sea-level and for the various sea-level contributors are addressed  
63 in this paper. Among these contributors, wind-waves play an important role on sea level at the  
64 coast (for a full discussion see Dodet et al., this issue), either directly, or indirectly through  
65 their influence on the wind stress and storm surge (e.g. Mastenbroek et al. 1993, Pineau-Guillou  
66 et al. 2018), and their role on the morphodynamic evolution of the nearshore (Coco et al., 2014;  
67 Masselink et al, 2016). Over the ocean shelves and along the coasts, ocean mass variations,  
68 reflected in ocean bottom pressure changes, are one of the dominant components of sea-level  
69 variability. These barotropic processes can be forced by either local or remote atmospheric  
70 pressure and wind variations, including travelling signals over the shelves or from the deep  
71 ocean. Unlike over shallow waters, the major contributor to sea-level changes in the open  
72 ocean, from seasonal to decadal time scales, is steric (density-driven) sea level (Meysignac et  
73 al., 2017). Steric sea level in the deep ocean is also relevant to the coastal zone, as these signals  
74 can propagate towards shallow waters through various mechanisms (Calafat et al., 2018;  
75 Hughes et al., this issue). Thus, hydrographic measurements are also important for the  
76 understanding of coastal sea-level variability. Such data, together with other ancillary  
77 observations (e.g. surface meteorology), through direct analysis or ingestion in assimilation  
78 systems, can significantly inform our ability to simulate and predict coastal sea level.

79 The aim of this work is to provide an overview of the current sea-level observing systems  
80 focusing on the coastal zone, as well as other complementary data sets that provide insight into  
81 some of the physical processes that drive sea-level variability. In section 2, we first describe  
82 the present status of the global tide gauge network and the data availability. We underscore the  
83 need of a continuous monitoring of vertical land motion at tide gauge stations and highlight its  
84 relevance for the complementarity between tide gauges, space geodetic techniques and coastal  
85 satellite altimetry, forming an integrated coastal sea-level observing system. Other emerging  
86 sea-level observing platforms that overcome some of the limitations of tide gauges are also  
87 described in section 3. In section 4, we describe the capabilities of wind-waves observing  
88 systems, whose effects at the coast are generally not captured by tide gauges. Sections 5 and 6

89 address ocean bottom pressure and hydrographic measurements, as observations needed to  
90 understand two major contributors to sea-level variability.

## 91 **2. Coastal sea-level observations: tide gauges and satellite altimetry**

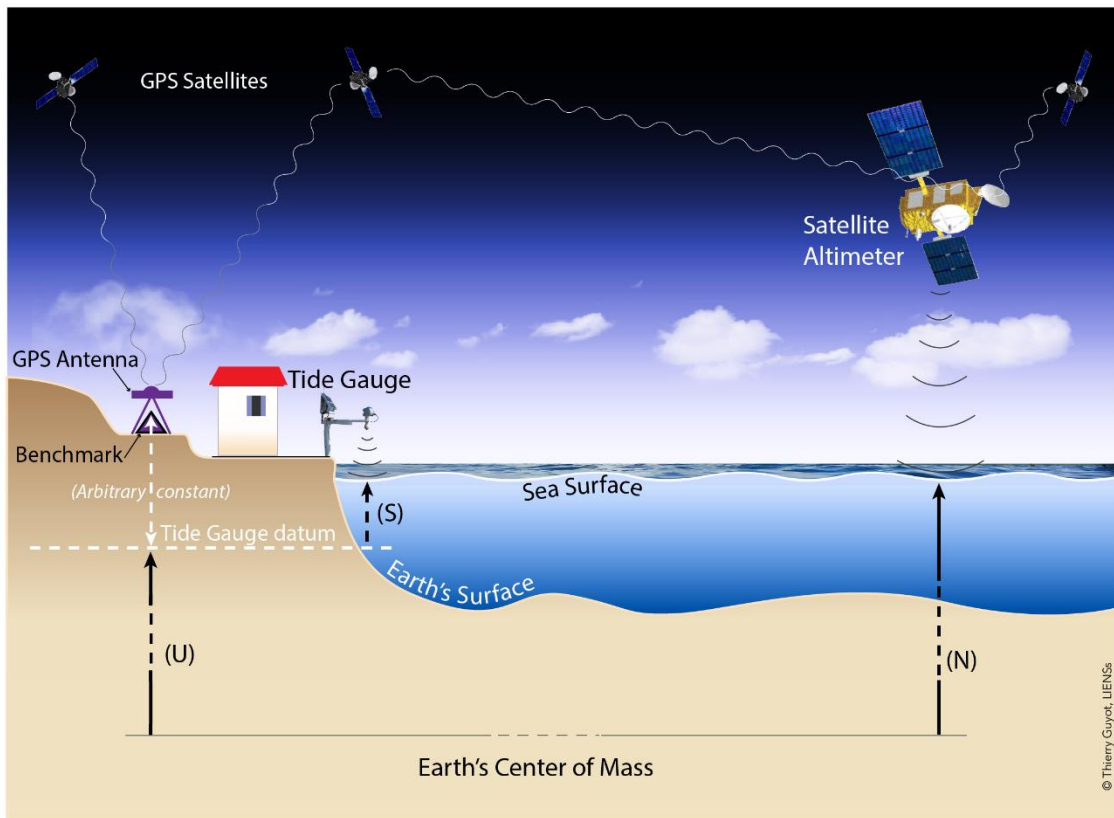
92 Tide gauges are the primary source of coastal sea-level observations, providing point-wise  
93 measurements of relative mean sea level and extreme sea levels (Intergovernmental  
94 Oceanographic Commission -IOC-, 1985). Initially designed for maritime navigation purposes,  
95 some of the oldest tide gauge records date back to the 18<sup>th</sup> century (e.g. Woodworth and  
96 Blackman, 2002; Woppelmann et al., 2006). These earliest sea-level observations were  
97 measured with tide poles and registered the time and height of tidal high and low waters (e.g.  
98 Woodworth and Blackman, 2002). Since the 19<sup>th</sup> century, stilling well floating gauges have  
99 become the most used technology and still represent the majority of the available records (Pugh  
100 and Woodworth, 2014); while originally recording sea-level oscillations in tidal charts, during  
101 the 20<sup>th</sup> century they have been upgraded to provide digital storage and transmission of data.  
102 New tidal stations tend to use radar gauges that measure the distance above the sea surface by  
103 analysing the time-of-flight of an electromagnetic reflected pulse. This type of gauge is  
104 nowadays preferred since it is relatively cheap, easy to install, and able to measure at high  
105 frequencies with the required accuracy and long-term stability (Martín Míguez et al., 2008).

106 Tide gauges measure relative sea level with respect to the land upon which they are grounded  
107 (Figure 1). Thus, to ensure continuity of the sea-level record, tide gauge measurements must  
108 refer to a properly defined datum, generally a fixed point on land referred to as tide gauge  
109 benchmark. Continuity can be achieved by systematically measuring the stability of the tide  
110 gauge benchmark through high precision levelling with nearby land points that are, ideally,  
111 tied to the corresponding national geodetic network. In addition, neither the height of the  
112 benchmarks nor the sea-level are constant but change at different spatial and time scales;  
113 therefore, precise estimates of the long-term vertical land motion are necessary in order to  
114 disentangle the land and ocean contributions to sea-level change in tide gauge records.

115 Currently, space geodetic techniques provide the most accurate way to measure vertical land  
116 motion (VLM) at tide gauge benchmarks. Among the Global Navigation Satellite Systems  
117 (GNSS), the most common is the Global Positioning System (GPS), a cost-effective, easy to  
118 install and maintain and high performance observing system (Figure 1). Woppelmann et al.  
119 (2007) published the first global-scale GPS vertical velocity estimates focused on the impact  
120 of VLM at tide gauges a decade ago and, since then, GPS estimates of VLM have been  
121 progressively incorporated into sea-level studies (Woppelmann and Marcos, 2016). VLM  
122 stems from different sources, either anthropogenic (e.g., ground water extraction) or natural  
123 (e.g., Glacial Isostatic Adjustment- GIA) and over multi-decadal to centennial time scales, they  
124 may display comparable values to those of the climate-related contributions to sea-level  
125 change.

126 Presently, the two biggest limitations of GPS-derived VLM corrections for global mean sea  
127 level are the accuracy of the reference frame on which they rely on (Santamaría-Gómez et al.,  
128 2017) and the shorter length of the GPS series compared to that of the tide gauges. In those  
129 cases where VLM at the tide gauge can be assumed to be constant, GPS VLM corrections reach  
130 an accuracy one order of magnitude smaller than sea-level trends from climate processes and  
131 therefore allow the reliable estimation of absolute sea level changes wherever both  
132 measurements are available (Woppelmann and Marcos, 2016). In contrast, limited knowledge  
133 of VLM at a tide gauge site can seriously bias the detection of long-term climate signals and  
134 hampers the assessment of climate impacts associated with long-term sea-level rise. The  
135 international program Global Sea Level Observing System (GLOSS, [www.gloss-sealevel.org](http://www.gloss-sealevel.org)),

136 in recognition of this need, recommends the installation of GNSS stations co-located with tide  
137 gauges.  
138

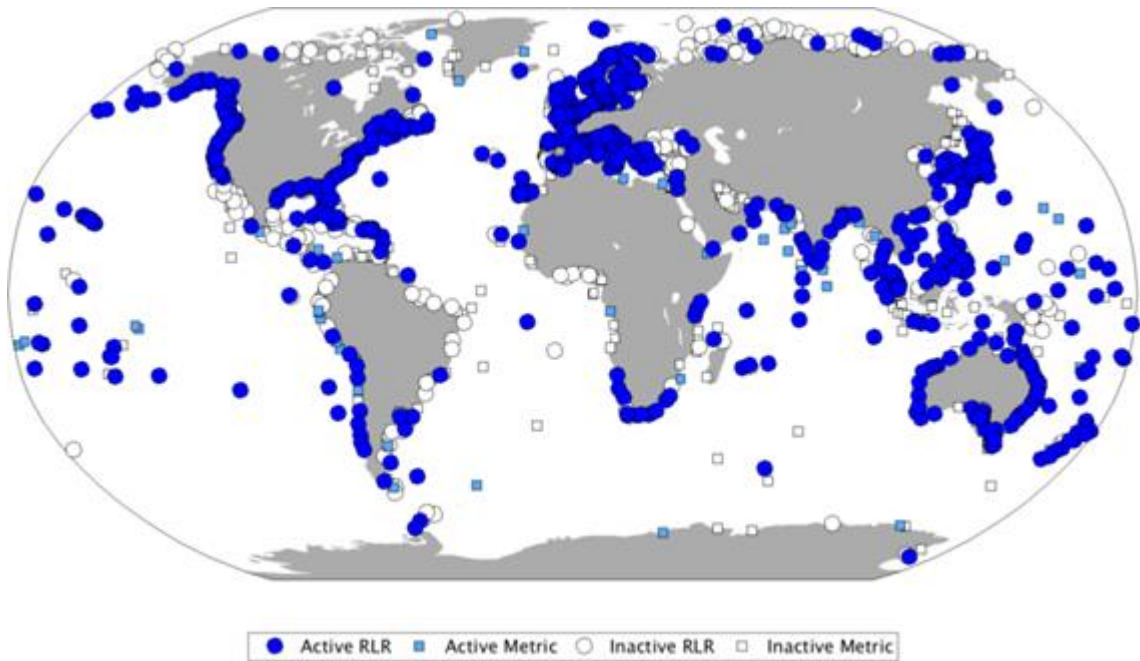


139  
140  
141  
142  
143

Figure 1. Sketch showing basic observational quantities and techniques associated with sea level measurement discussed in this article

144 Sea-level records from tide gauges are stored in and distributed by international databases. The  
145 most extensive data bank of long-term mean sea level changes from tide gauges is the  
146 Permanent Service for Mean Sea Level (PSMSL, psmsl.org), hosted by the National  
147 Oceanography Centre in Liverpool and founded in 1933. PSMSL distributes monthly mean sea  
148 level records compiled from several national and subnational agencies worldwide (Holgate et  
149 al., 2013) and currently hosts more than 2000 tide gauge stations, of which 1023 are active  
150 (defined as those with data supplied to PSMSL in 2013 or later) (Figure 2). To be useful for  
151 climate studies, sea-level records must refer to a consistent datum; these are termed as Revised  
152 Local Reference (RLR) in the PSMSL data set and represent 64% of the total number of  
153 stations. Despite the present-day global picture mapped in Figure 2 that shows a good spatial  
154 tide gauge coverage of the world coastlines, this has not always been the case in the past  
155 decades and century. Only a small subset of 89 tide gauge records span more than 100 years  
156 (Figure 3), and these stations are mainly concentrated along the historically more developed  
157 coastlines, mostly in Europe and North America. The number of tide gauge records increases  
158 significantly since the mid-20th century (Holgate et al., 2013), although, again, with most  
159 stations being located in the Northern Hemisphere (Figure 3).

160

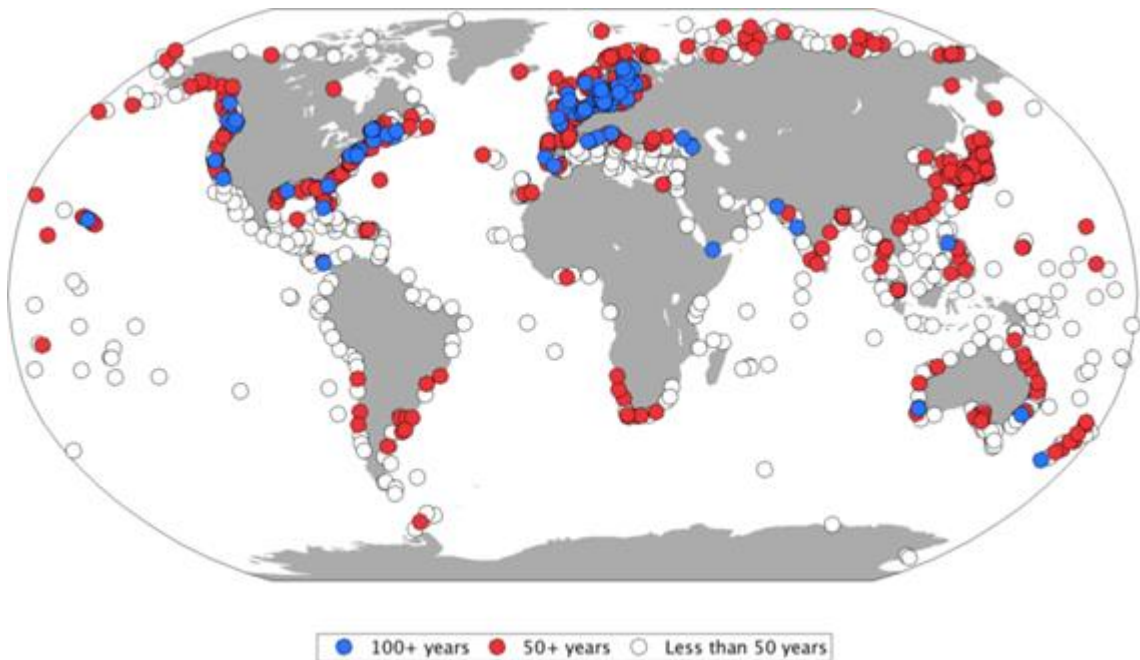


161

162 Figure 2. Tide gauge stations in the PSMSL database. Active stations (in blue) are defined as  
 163 those with data supplied to PSMSL in 2013 or later. Stations with historical levelling  
 164 information are identified as Revised Local Reference (RLR).

165

166



167

168 Figure 3: RLR tide gauge records longer than 100 (blue) and 50 (red) years, not accounting for  
 169 data gaps.

170

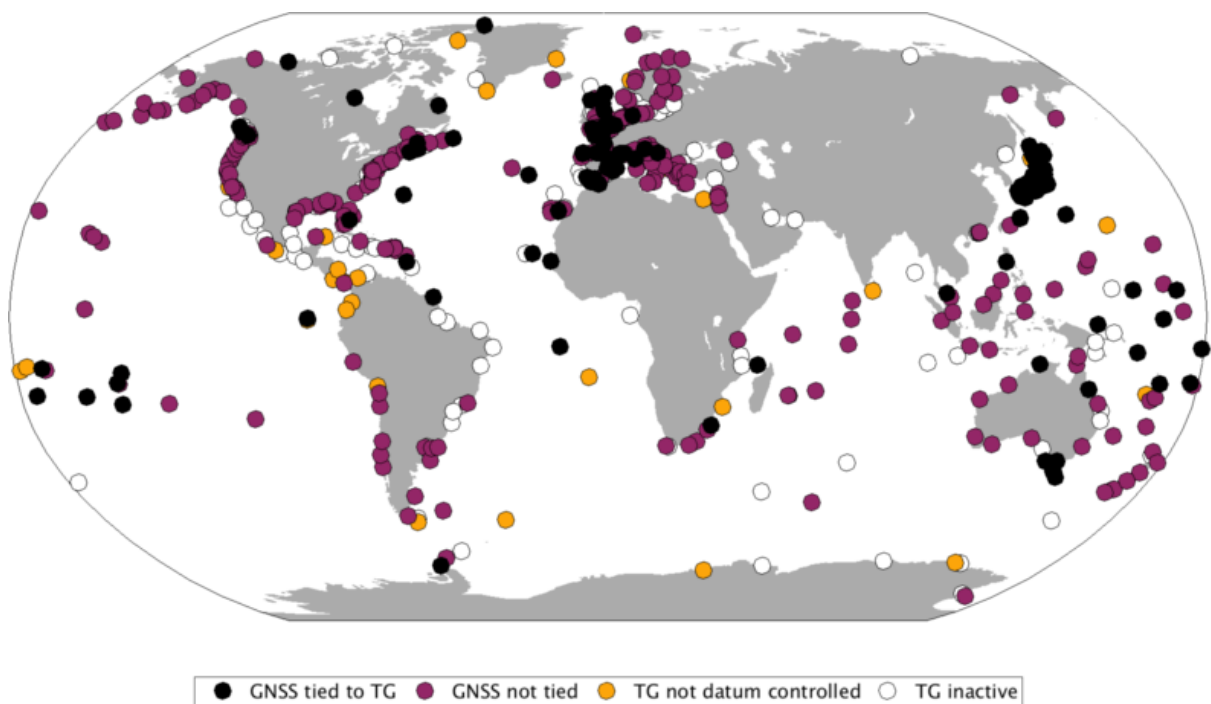
171 The uneven spatial and temporal distribution of tide gauge records and, in particular, the  
 172 scarcity of data during the early 20<sup>th</sup> century and before, are factors that hinder the  
 173 quantification and understanding of past regional and global long term mean sea level changes

174 and their driving mechanisms (Dangendorf et al., 2017). Many efforts have therefore been  
175 devoted to the discovery, recovery and quality control of historical archived sea-level  
176 measurements (Bradshaw et al., 2015; Hogarth, 2014). These so-called exercises of data  
177 archaeology have successfully recovered sea-level information at sites as remote as the  
178 Kerguelen Islands (Testut et al., 2006) or the Falklands (Woodworth et al., 2010) and as far  
179 back in time as the 19<sup>th</sup> century (Talke et al., 2018; Woppelmann et al., 2014; Marcos et al.,  
180 2011). Tide gauge data archaeology has been a useful tool to recover sea-level measurements  
181 valuable for climate studies, given the potential to expand the databases during periods and in  
182 places where no other observations exist.

183 Another major factor that hampers the understanding of contemporary sea-level changes is the  
184 limited knowledge of VLM at tide gauges during the last century. Before the maturity of the  
185 GNSS observations, the only VLM being accounted for in sea level studies was GIA, as it can  
186 be modelled with prescribed ice history and solid Earth properties (e.g. mantle viscosity). With  
187 the development of high precision GNSS, VLM is nowadays estimated from observations.  
188 Global GPS velocity fields are routinely computed and distributed by a number of research  
189 institutions (International GNSS Service, Jet Propulsion Laboratory, University of Nevada,  
190 University of La Rochelle). Among these, only the French SONEL (Système d'Observations  
191 du Niveau des Eaux Littorales) data centre, hosted at the University of La Rochelle, provides  
192 GPS observations and velocity estimates focused on the coastal areas and tide gauge stations,  
193 thus being closely linked to PSMSL and forming an integrated observing system within the  
194 GLOSS program. Unfortunately, and despite the GLOSS recommendations, only a limited  
195 number of tide gauges is co-located or tied to a nearby GNSS station (Figure 4). In particular,  
196 in the PSMSL database only 394 RLR stations are within a 10km distance from a GNSS station  
197 and, among these, only for 102 stations the levelling information between the two datums is  
198 available, which is a serious limitation for some applications such as studies on the ocean  
199 dynamic topography (Woodworth et al., 2015).

200

201



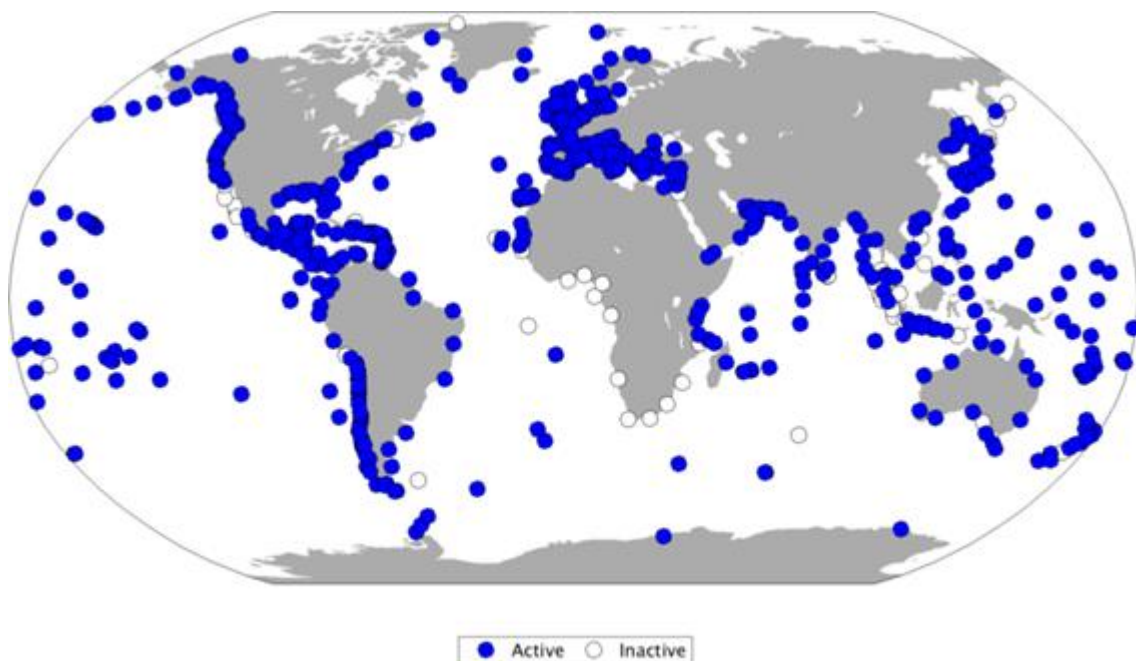
203 Figure 4. GNSS stations with (coloured) and without (blank) a tide gauge within 10 km,  
204 according to PSMSL and SONEL databases [data accessed on 3 September 2018]. Black dots  
205 indicate RLR stations where GNSS and tide gauge datum are tied, purple dots indicate  
206 otherwise. Orange stations have no information about the tide gauge datum continuity (metric  
207 stations).

208

209 Coastal mean sea level can be also obtained from other data portals. These include the European  
210 Copernicus Marine Environment Monitoring Service (CMEMS, <http://marine.copernicus.eu/>),  
211 the University of Hawaii Sea Level Center (UHSLC, <https://uhslc.soest.hawaii.edu/>) and  
212 numerous national data services. For long-term sea-level studies they provide mostly data that  
213 is also available in PSMSL. In addition, some of them distribute high frequency (hourly and  
214 higher) sea-level measurements required for the study of tides and extremes and/or real time  
215 measurements needed for purposes such as operational oceanographic services or tsunami  
216 monitoring and warning systems. The Flanders Marine Institute (VLIZ, [www.vliz.be/en](http://www.vliz.be/en)) hosts  
217 the GLOSS sea level monitoring facility for real time data. Of a total of 993 tide gauge stations  
218 currently hosted and distributed by VLIZ (Figure 5), 856 are active (defined here as those  
219 stations that have supplied data in 2018). The UHSLC hosts two subsets of high frequency sea  
220 level observations: one termed as fast delivery for operational purposes and another one of  
221 research quality in which the same data have undergone a quality control process. The Global  
222 Extreme Sea Level Analysis initiative (GESLA, [www.gesla.org](http://www.gesla.org)) extends the UHSLC high  
223 frequency sea level data set unifying and assembling delayed-mode observations compiled  
224 from national and sub-national agencies. The GESLA data set is presently the most complete  
225 collection of high-frequency sea level observations, with 1355 tide gauge records (Woodworth  
226 et al., 2017).

227

228



229

230 Figure 5. Tide gauge stations providing real time sea level observations to VLIZ data centre.  
231 Active stations are defined as having contributed data in 2018.

232

233 In addition to the tide gauge monitoring, sea-level variations are also continuously measured  
234 by high-precision satellite altimetry with quasi global coverage since 1992 (Figure 1). The  
235 constellation of altimetry missions over the last 25 years will be continued with operational  
236 missions in the future (see Vignudelli et al., this issue). Near coastlines, the sea-level data  
237 retrieval and interpretation from altimetry measurements become particularly complex.  
238 However, in the last decade there have been important advances that have extended the  
239 capabilities of satellite altimetry for the observation of coastal sea level: great progress has  
240 been made in altimeter instruments (CryoSat-2, AltiKA, Sentinel-3A&B) and also in the  
241 processing algorithms and products (see Vignudelli et al., this issue, for more details). Although  
242 there is still a gap of information in a coastal band a few kilometres wide, this is continuously  
243 reduced thanks to the efforts invested by the altimetry community. Nowadays, sea-level data  
244 derived from satellite altimetry are available generally up to 5-10 km from the coastline, much  
245 closer than only a few years ago (Biol et al., 2016). Thus, altimetry data is now providing very  
246 valuable information for coastal sea level studies (Cipollini et al., 2017) and it is expected that  
247 it will become an additional source of long-term sea-level observations, which will be  
248 especially relevant in coastal zones where in-situ data are inexistent or scarce.

249 Tide gauges and satellite altimetry have different spatial and temporal sampling. Radar  
250 altimeters measure sea level along the satellite ground tracks every 6 km and with a typical  
251 distance between the ground-tracks of 50–300 km (depending of the number of satellites in the  
252 altimeter constellation). Several projects are currently generating data at a higher rate  
253 (corresponding to along-track distances of 175-350 m) with dedicated algorithms. The revisit  
254 time of observations is a few days. Although not (yet) available up to the coastline, altimeter  
255 data offer a nearly-global regular spatial sampling from the deep ocean to part of continental  
256 shelves (sometimes a large part), and thus a regional view of ocean dynamics. In contrast, tide  
257 gauges measure sea level every few seconds or minutes but only at a single coastal point, often  
258 at relatively sparse locations. The two data sets are therefore complementary and often  
259 integrated to maximise the information they provide (Figure 1).

260 One major difference between the two data sets is the geodetic reference frame to which they  
261 are related. Tide gauges provide relative sea level while satellite altimetry measures ‘absolute’  
262 sea level variations with respect to a reference ellipsoid. Levelling of the tide gauge benchmark  
263 by means of geodetic methods is thus necessary if altimetry and tide gauge absolute sea levels  
264 are to be compared.

265 As a final remark, it is worth mentioning that relative comparisons between satellite altimeter  
266 and tide gauge observations are essential to evaluate the long-term stability of satellite  
267 altimetry. They are also systematically used to evaluate and validate new altimeter missions,  
268 data processing algorithms and products. In that sense, both types of sea level observations can  
269 again be considered as two components of the same global observing system.

### 270 **3. Other sea-level monitoring platforms**

271 In addition to extensively used tide gauge and altimetric observations, coastal sea level is also  
272 monitored by emerging GNSS-based methods. These observing systems have benefited from  
273 progress in GNSS data processing. In particular, the development of GNSS Precise Point  
274 Positioning in kinematic mode with integer ambiguity fixing allows for centimetre accuracy  
275 (Laurichesse et al., 2009; Fund et al., 2013) without the need of a reference station. Some of  
276 these new systems are reviewed here. They provide complementary measurements, often  
277 designed for particular purposes and locations.

278 Taking advantage of GNSS co-location with tide gauges, GNSS radio signals reflected from  
279 the sea surface have been used recently to estimate coastal mean sea level, with daily mean

280 differences of a few cm with respect to conventional tide gauges (Larson et al., 2013). The  
281 GNSS reflectometry technique provides an alternative coastal sea-level observing system with  
282 important advantages: coastal mean sea level is measured directly in a geocentric frame  
283 consistent with satellite altimetry; it does not require in-situ calibration; the vertical tie between  
284 the GNSS antenna and a nearby tide gauge can be done remotely and continuously, i.e., it  
285 allows monitoring the stability of the tide gauge zero (Santamaría-Gómez and Watson, 2016).  
286 With the new GNSS constellations (e.g. Galileo, Beidou) and the new and more precise signals  
287 (e.g. AltBOC, Fantino et al., 2008), this technique will improve precision and sampling rates,  
288 maximizing the benefit of co-location with tide gauges.

289 Another example is the use of GNSS, in particular GPS, on floating devices that emerged with  
290 the birth of precise satellite altimetry and the subsequent need for in-situ data calibration. These  
291 data provided estimates of the absolute bias of the altimetry system, which is critical to monitor  
292 its long-term stability and assess sea-level trends. First GNSS buoys were developed for the  
293 absolute calibration of TOPEX/Poseidon (Hein et al., 1990; Rocken et al., 1990; Born et al.  
294 1994). Since then, many different designs have been proposed to ensure a centimetric sea level  
295 height measurement and reduce the impact of the inherent limitation of the system (Figure 6),  
296 such as the ease and duration of deployment, the quantification of the height of the GNSS  
297 antenna phase centre above the water line and the tilt of the antenna from vertical. The results  
298 from an inter-comparison of different GNSS buoy designs carried out at Aix Island (west coast  
299 of France) in 2012 showed that these devices are able to measure the absolute sea level height  
300 with cm-level accuracy, thus being comparable to the precision of the reference radar tide  
301 gauge (André et al., 2013). GNSS buoys are now routinely used in dedicated satellite altimetry  
302 calibration sites such as Corsica Island in the Mediterranean Sea (Bonfond et al., 2003a),  
303 Bass Strait in southern Australia (Watson et al., 2003) and now the Harvest Platform in the US  
304 Pacific coast (Haines et al., 2017). They are also used for tide gauge error characterization and  
305 calibration (Watson et al., 2008; Martín Míguez et al. 2012; André et al., 2013) and vertical sea  
306 floor height monitoring (Ballu et al., 2010).



307  
308 Figure 6. Illustration of four different GNSS buoy designs. Top left and right are respectively  
309 buoys designed at DT-INSU and IGP (André et al., 2013). Lower left is a new light buoy  
310 design by DT-INSU based on the blanket concept to closely follow the water surface. Lower

311 right buoy is the buoy used at Bass Strait (Australia) for altimetry calibration studies (Watson  
312 et al. 2008).

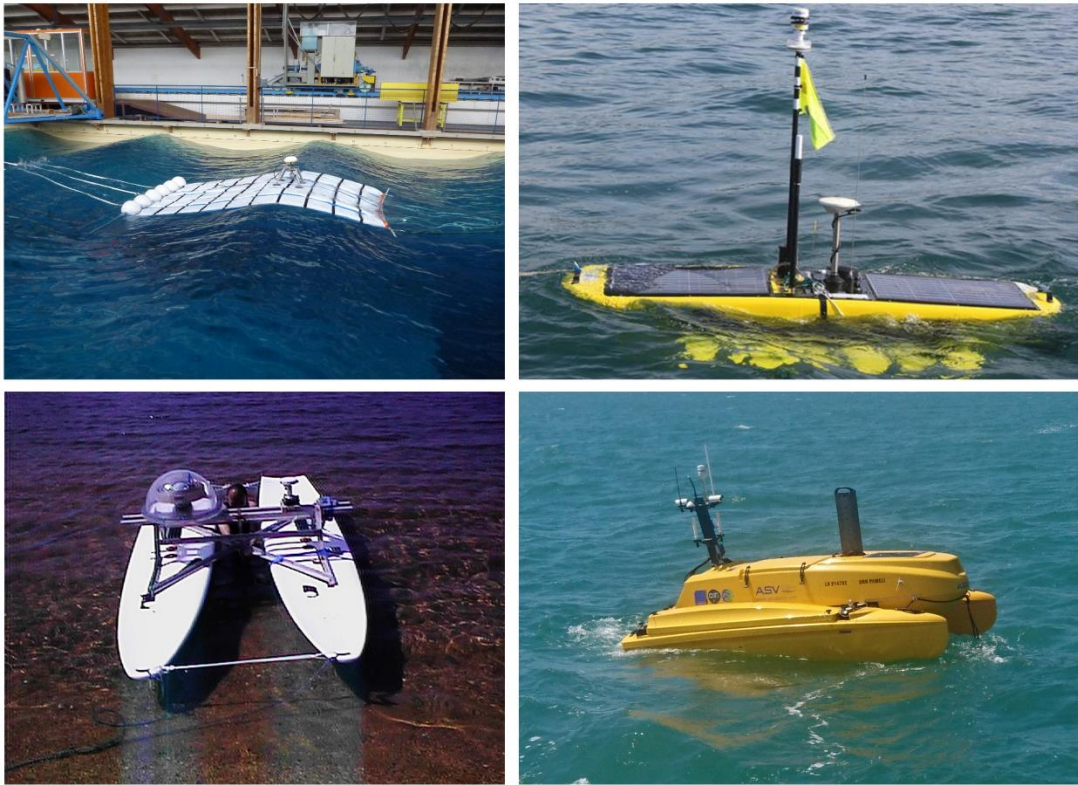
313

314 Rather than pointwise measurements, mapping spatial variations of sea surface height in coastal  
315 areas brings invaluable information on the local geoid as well as for hydrodynamic processes.  
316 These variations cannot be properly apprehended by tide gauges or GNSS buoys, nor by  
317 satellite altimetry due to the proximity to land and limited spatial and temporal sampling. Sea  
318 surface height mapping has been carried out so far using GNSS equipped boats or towed  
319 platforms to retrieve local geoids (Bouin et al., 2009a). Such efforts have been used, for  
320 instance, in calibration/validation altimetry studies, both to get the geoid height difference  
321 between the reference tide gauge and the nearby satellite track and to increase the quality of  
322 the altimetry processing by better accounting for along and across-track gradients (Bonfond  
323 et al. 2003b). A major issue for these measurements carried while moving is the monitoring of  
324 the GNSS antenna air-draft (elevation difference between the above water GNSS antenna and  
325 the water level), which can vary with the load or speed of the measuring platform (Bouin et al.  
326 2009b; Foster et al., 2009; Reinking et al., 2012). To overcome this limitation, a new  
327 measurement system based on a towed blanket has been proposed, which ensures a perfect  
328 coupling between the floating device and the sea surface and therefore, a constant GNSS  
329 antenna height above water. The device is a floating blanket made of foam boards assembled  
330 with marine fabrics; the GNSS antenna is mounted on the blanket using a tripod, and its  
331 verticality while in motion is achieved using a gamble system (see Figure 7). A number of tests  
332 of this design have been carried out under various conditions (Bangladesh, Aix Island and  
333 Corsica in France, Kerguelen) with successful results (Calzas et al., 2014; Durand et al., 2017).

334

335 Another alternative system to map spatial variations in sea surface height arises with the  
336 development of Autonomous Surface Vehicles (ASV). For example, Penna et al. (2018) used  
337 a self-propelled Wave Glider (built by Liquid Robotics) equipped with a GNSS recording at  
338 5Hz to cover a distance of 600 km in 13 days with centimetric precision. This system proves  
339 its efficiency for offshore areas; however, with over 6m of water-draft and a manoeuvrability  
340 highly dependent on weather conditions, it is not suitable for shallow coastal waters and areas  
341 with heavy maritime traffic. In contrast, the University of La Rochelle and DT\_INSU (Division  
342 Technique de l'Institut National des Sciences de l'Univers) are currently developing a  
343 measurement system, named PAMELi (Plateforme Autonome Multicapteur pour l'Exploration  
344 du Littoral, Ballu et al., 2017), integrating a continuous air-draft quantification to be installed  
345 on a C-CAT3 built by ASV Global company (<https://www.asvglobal.com/product/c-cat-3>).  
346 Unlike the Wave Glider, this system can also measure sea surface heights in shallow waters  
347 and should be suitable for zones with significant maritime traffic thanks to its remotely  
348 operating capabilities that include real-time camera viewing. The interest of such systems  
349 compared to the towed blanket is both its compactness/manoeuvrability and its ability to be  
350 used as a multi-sensor platform for an integrated study of the dynamics of coastal waters. For  
351 instance, the PAMELi platform will be able to continuously monitor en-route temperature,  
352 salinity, turbidity, chlorophyll, bathymetry, atmospheric parameters in addition to mapping sea  
353 surface height (Coulombier et al., 2018). Such mobile devices will be key for in-situ calibration  
354 of future wide-swath satellite altimeters and validation of coastal hydrodynamical models.  
355 Integrated systems will contribute to better monitorization and interpretation of sea surface  
356 height variations at short temporal and spatial scales.

357



358

359 Figure 7. Illustration of moving GNSS platform for sea surface height mapping (towed blanket  
 360 (Calzas et al., 2014), Wave-glider (Penna et al. 2018), Catamaran (Bonfond et al., 2003b),  
 361 and AUV-PAMELi (Coulombier et al., 2018)

362

#### 363 4. Wind-wave observations

364 Direct wave effects on coastal sea level exist at all time scales, from a mean sea level response,  
 365 known as wave set-up, to the swash and possible overtopping lasting only a few seconds (Dodet  
 366 et al., this issue). Intermediate time scales are dominated by infragravity waves with typical  
 367 periods of 30 to 300 s. Due to the range of spatio-temporal scales, the observational  
 368 requirements for accurately monitoring these processes are different. Furthermore, all these  
 369 effects of waves on the sea level are concentrated in the “surf zone” where the along-shore  
 370 variability can be very large as the sea state is strongly influenced by the bathymetry (Munk  
 371 and Traylor 1947, Magne et al., 2007), bottom types (e.g. Ardhuin et al., 2002; Lowe et al.,  
 372 2007; Monismith et al., 2017) and currents (e.g. Battjes 1982; Ardhuin et al. 2017). As a result,  
 373 only specific surf zone locations have been equipped with routine continuous measurements  
 374 (including wave height, period and direction), as it is today impossible to monitor the strong  
 375 alongshore variability of the wave impacts.

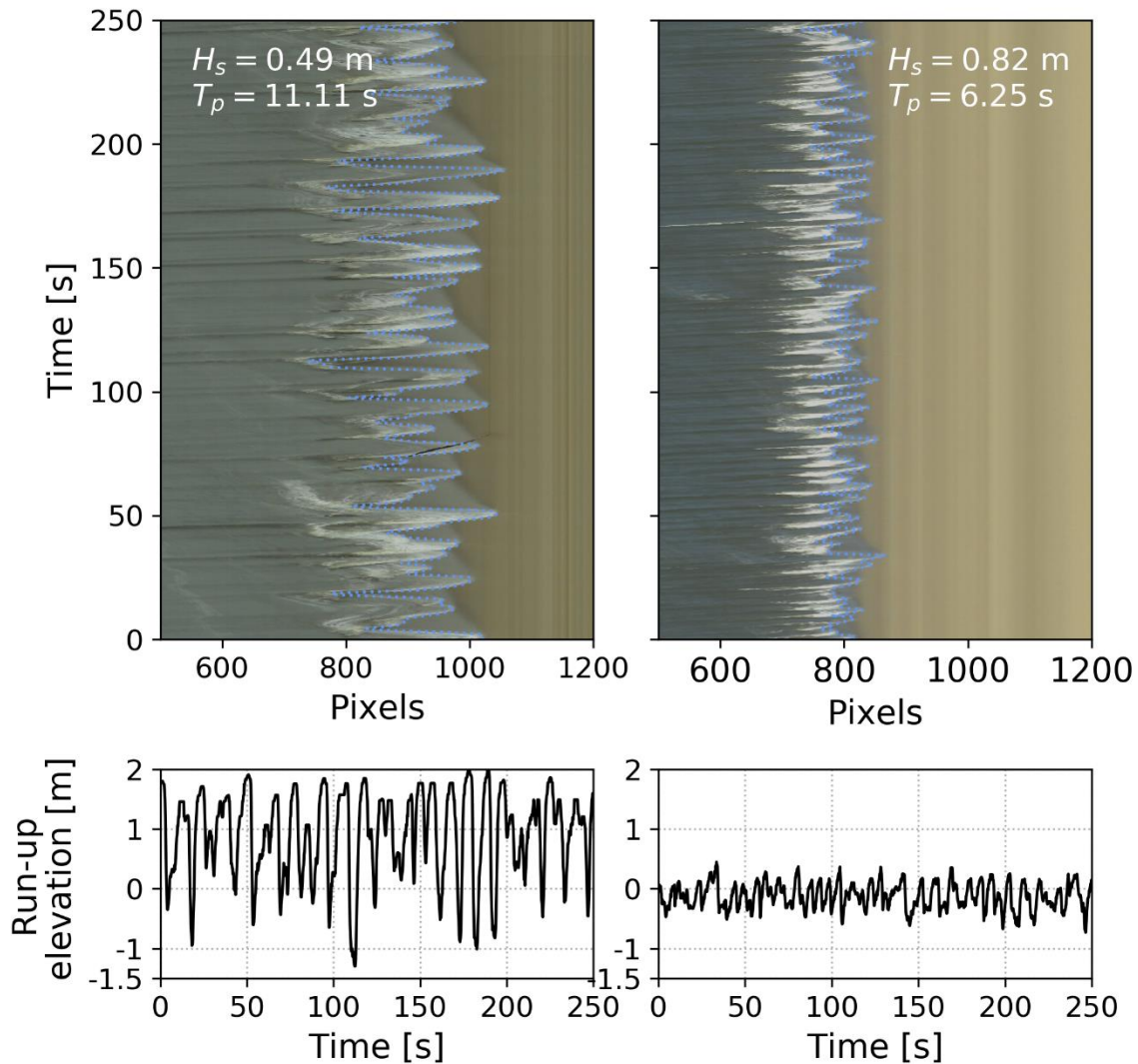
376 Surf zone processes have been the topic of targeted instrument deployments (e.g. Guza and  
 377 Thornton 1981; Egar et al., 1997; Senechal et al., 2011a). Such experiments have confirmed  
 378 that the wave set-up is caused by the cross-shore convergence of the wave-induced momentum  
 379 flux, known as the radiation stress (e.g. Raubenheimer et al., 2001). This balance is also  
 380 perturbed by bottom friction in the shallowest regions (Apotsos et al. 2007). Wave set-up, just  
 381 like wave transformation in general, is strongly influenced by the nearshore underwater  
 382 bathymetry (Stephens et al., 2011), which is problematic to measure directly (e.g., Dugan et  
 383 al., 2001) or indirectly (e.g., Holman et al., 2013). Despite their importance, measurements of  
 384 underwater bathymetry in the surf zone remain a challenge and at present such data is only

385 available at few sites and for short temporal intervals obtained through in-situ surveys. The  
386 development of remote sensing techniques from high resolution radar or optical satellite  
387 imagery (e.g. Pleskachevsky et al. 2011) now benefits from faster revisits using Landsat 8 and  
388 Sentinels 1 & 2 (Hedley et al. 2012) but bathymetric changes during storms, which are larger  
389 and most relevant, are still inaccessible.

390 The “infragravity” oscillations of the sea level at the scale of a few minutes are associated to a  
391 more complex balance with a transfer of energy from the wind-waves that is influenced by the  
392 varying water depth (see Bertin et al., 2018 for a review). Infragravity (IG) wave heights are  
393 generally proportional to the wind-wave height but that proportionality factor varies  
394 considerably with the depth profile, with larger proportionality factors on steep slopes  
395 (Sheremet et al., 2014). Measurements of IG waves have been relatively few so far. Right at  
396 the shoreline, the large variation of the cross-shore IG wave height is generally poorly captured  
397 by a sparse array of pressure gauges and current meters (e.g., Raubenheimer, 2002). Offshore  
398 pressure gauges can provide a region-integrated measurement of IG waves at the coast as they  
399 propagate offshore (e.g. Rawat et al., 2014; Neale et al., 2015). The other extreme is given by  
400 high frequency tide gauge data, usually from harbours. These are purely local measurements  
401 in which the IG frequency band can be strongly amplified into seiches by harbour resonances  
402 (e.g. Okihiro et al., 1993; Ardhuin et al., 2010). All these measurements only offer a few proxy  
403 of the IG amplitudes on the open coast and just at a few selected locations.

404 Other observation systems of wind-waves include, in daylight, routine monitoring techniques  
405 based on video imagery that have been perfected over the past 30 years (e.g. Holman and  
406 Stanley, 2007). As video instrumentation, data storage and processing time are becoming  
407 cheaper, video records are now included in many coastal monitoring programs (e.g.,  
408 <http://ci.wrl.unsw.edu.au/> and Figure 8) and used to study wave runup, also during extreme  
409 events (Senechal et al., 2011b). Recent experiments with Lidar are an interesting alternative  
410 for all-weather surveys of beach transects (Fiedler et al., 2015). Other sparse surveying  
411 strategies have also used photography and high-water marks (Cariolet and Suanez, 2013). Such  
412 measurements have provided extensive datasets that form the basis of empirical formulas  
413 linking, mean, IG and extreme sea levels to “offshore” wave parameters, generally the  
414 significant wave height, mean period and beach slope (Stockdon et al., 2006).

415



416

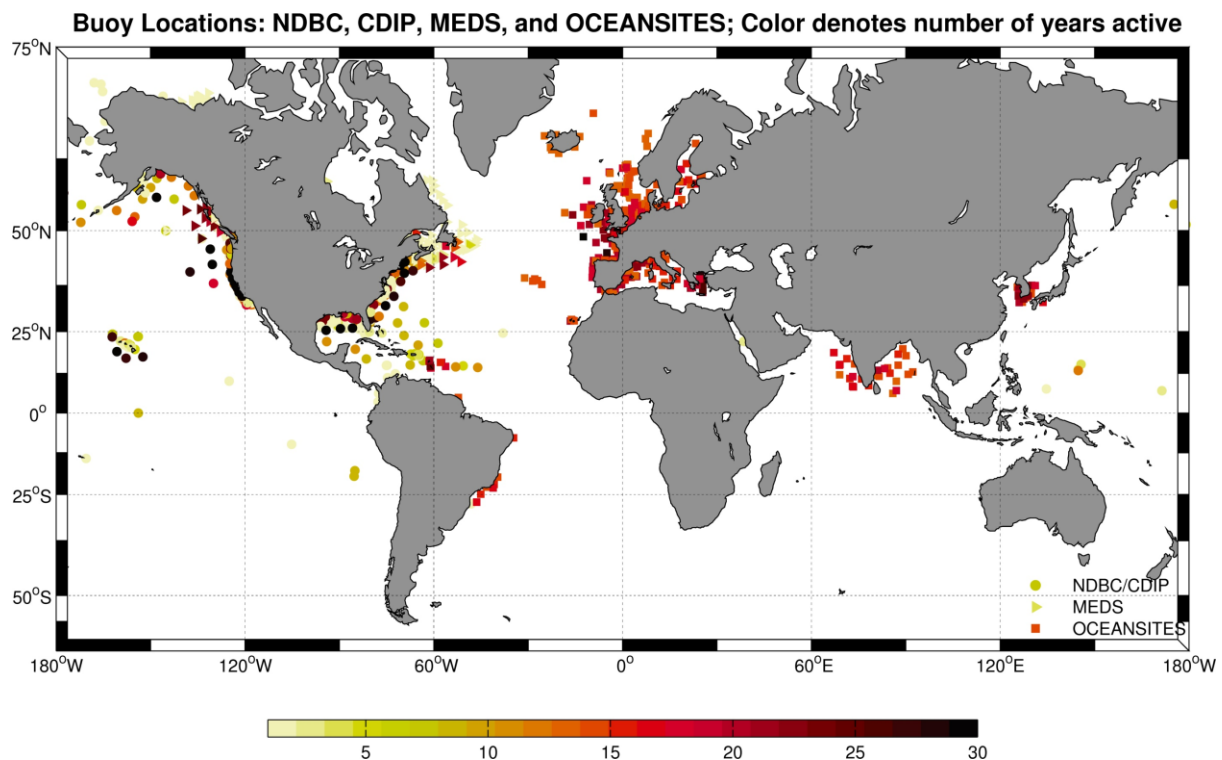
417 Figure 8. Examples of time stacks showing shoreline position over time (top panels) during  
 418 (left) high and (right) low tide. The corresponding significant wave height ( $H_s$ ) and wave peak  
 419 period ( $T_p$ ) are indicated for each case. Bottom panels show the detrended runup elevation time  
 420 series. Observations collected at Bunkerhill Beach, Sylt, Germany (courtesy of J. Montano).

421

422 Whatever the wave transformations and impacts along the coast, there is an evident need for  
 423 observations on offshore sea state parameters that trigger those effects. The longest time series  
 424 are available for wave heights from in-situ measurements using voluntary observing ships  
 425 (Gulev et al., 2003) and buoys (Figure 9) and from satellite altimeters (Queffeulou, 2013).  
 426 Conversely, the routine measurement of wave periods is limited to the few available buoys or  
 427 platforms (Figure 10). To overcome this limitation, proxies for a mean wave period have been  
 428 proposed using radar backscatter and wave heights from altimeters (e.g. Gommenginger et al.  
 429 2003; Quilfen et al., 2004). It should be still investigated how well these proxies perform for  
 430 estimating extreme coastal sea levels. In the near future, it is expected that forthcoming  
 431 satellites will bring a direct measurement of the dominant period in most sea state. This is the  
 432 case of the SWIM instrument on CFOSAT (Hauser et al., 2017), to be launched in October  
 433 2018. The proposed SKIM satellite would go a step further in resolving the dominant waves  
 434 even in enclosed seas (Ardhuin et al., 2018). Still, even with a 300 km wide swath SKIM  
 435 would have a revisit time of 4 days at mid-latitudes that is insufficient to resolve the fast time

436 scale of storms. This large revisit time, compared to the typical time scale of 12 hours for storm  
437 duration, makes it impossible, from satellites alone, to derive reliable statistics on extreme  
438 wave parameters and associated impact on sea level.

439



440 Figure 9. Location of wave-measuring devices affiliated to the NDBC, CDIP, MEDS or  
441 OCEANSITES networks with the length of records in years indicated by the colours.

442

443 It should be emphasized that all these observations systems have not been designed for the  
444 analysis of wave impacts on sea level trends. Indeed, an increase in significant wave height by  
445 2 cm produces an increase in sea level by 0.5 to 6 cm on typical beaches, depending on  
446 shoreface slope, wave period and bed composition (Stockdon et al., 2006; Poate et al., 2016).  
447 As a result, a reasonable goal for the accuracy of trends on wave height is an accuracy lower  
448 than the mean sea level rise of 3 mm/year. This should apply to the extreme values, be it the  
449 95<sup>th</sup> percentile or a 10-year maximum wave height, depending on applications. This is more  
450 demanding than the existing requirement of 5 cm per decade that is today the goal listed by  
451 GCOS, but it is also much less than what has been achieved by studies of buoy data for which  
452 the accuracy is of the order of 3 cm/year (Gemrich et al., 2011).

### 453 5. Ocean bottom pressure observations

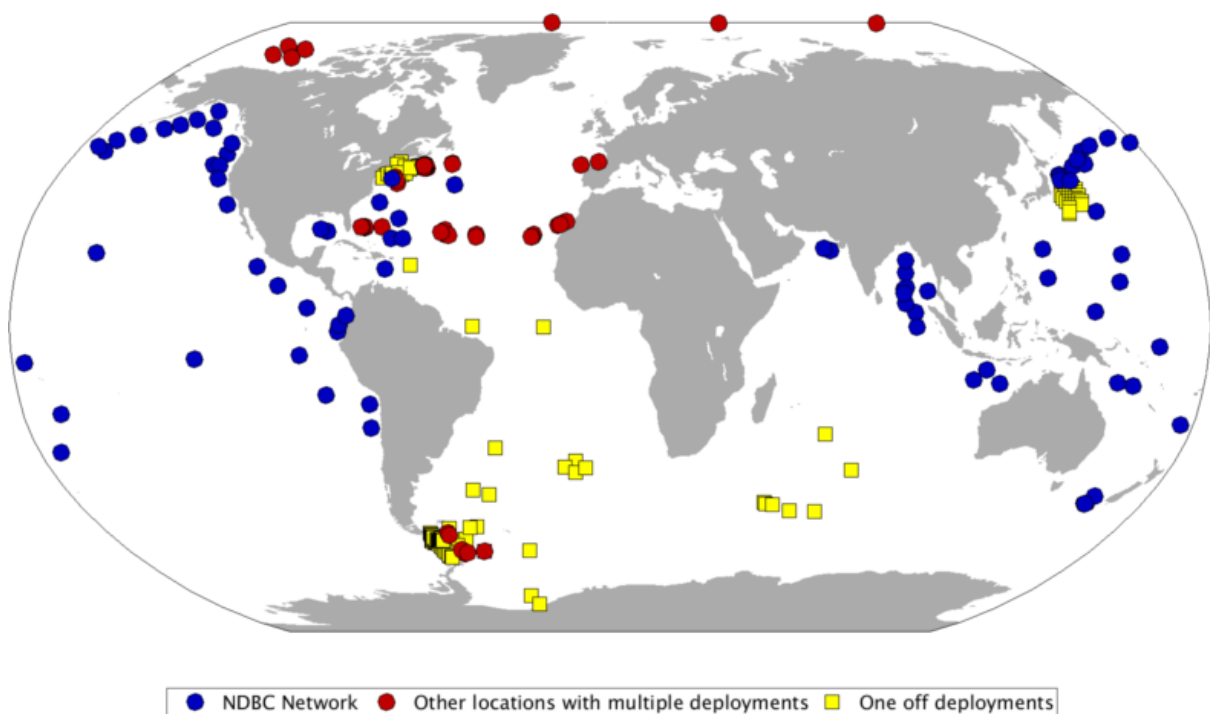
454 The first bottom pressure observations were motivated by the need to understand ocean tides,  
455 which was hampered by the lack of knowledge about tidal cycles in the open oceans, with tide  
456 gauges by definition located at the shore. Attempts began in the 1960s to measure the tides in  
457 the open sea using instruments capable of recording pressure accurately at the seabed  
458 (Cartwright, 1977). As the technology matured, programmes evolved to use a succession of  
459 deployments at a site to provide an ongoing record of sea level variation (Spencer et al., 1993),  
460 with a new sensor deployed to the seabed as the old one was recovered, along with its payload  
461 of data. Unfortunately, pressure sensors are prone to drift over time, best modelled with a  
462 decaying exponential in the short term and a linear drift in the long term (Watts and

463 Kontoyiannis, 1990; Polster et al., 2009). Although there have been some attempts to measure  
464 and correct the drift with in-situ calibration systems (e.g. Sasagawa et al., 2016), these are still  
465 under development and are not yet able to provide routine corrections.

466 As the drift cannot be distinguished from any long-term secular trends, and the information  
467 cannot be connected to a specific datum, records from bottom pressure gauges are presently  
468 unsuitable for monitoring long-term changes in sea level. Nevertheless, the records can be used  
469 to investigate changes in bottom pressure caused by tides (Ray, 2013), ocean circulation  
470 (Spencer et al., 1993), and ocean mass (Hughes et al., 2012). Furthermore, by pairing the sensor  
471 with a surface buoy capable of transmitting high frequency real time data, recorders can provide  
472 data in real time and thus be used as a vital part of regional tsunami monitoring networks  
473 (Meinig et al., 2005).

474 A substantial network of bottom pressure recorders (BPR) is maintained by NOAA, and data  
475 can be obtained from the National Data Buoy Center (NDBC) website ([www.ndbc.noaa.gov](http://www.ndbc.noaa.gov)).  
476 The PSMSL also distribute some bottom pressure data from various sources, including a subset  
477 of the NDBC data, and maintains a list of other available BPR data  
478 ([www.psmsl.org/data/bottom\\_pressure](http://www.psmsl.org/data/bottom_pressure)). Deployments tend to be clustered in locations where  
479 particular phenomena have been studied (such as the Drake Passage), or in tsunami-prone areas  
480 (Figure 10), leaving large areas of the ocean unobserved by these in-situ measurements.

481



482

483 Figure 10. Bottom pressure recorder measurements available from the NDBC and PSMSL  
484 networks, or other networks linked to by the PSMSL.

485

486 Satellite gravimetry, starting from the launch of the Gravity Recovery and Climate Experiment  
487 (GRACE) in March 2002, has demonstrated its usefulness for observing ocean bottom pressure  
488 variations in the deep ocean (Bergmann and Dobsław, 2012; Chambers and Bonin, 2012;  
489 Johnson and Chambers, 2013; Picuch et al., 2013; Ponte and Picuch, 2014; Makowski et al.,  
490 2015), and calculating the mass component of global mean sea level (Chambers et al., 2004;

491 Willis et al., 2008; Leuliette and Miller, 2009; Boening et al., 2012; Church et al., 2013; Fasullo  
492 et al., 2013; Johnson and Chambers, 2013; Rietbroek et al., 2016; Chambers et al., 2017). Using  
493 the newest release of GRACE data, bottom pressure in the deep, interior ocean averaged over  
494 a disk with radius 300 km has a standard error of approximately 1.5 cm of equivalent sea level  
495 (Chambers and Bonin, 2012), while the global ocean mass has a standard error of 1.1 mm  
496 (Johnson and Chambers, 2013), both at monthly averages.

497 Using GRACE data to accurately measure ocean bottom pressure (and hence, the mass  
498 component of sea level) in coastal waters is very difficult and, until recently, has only been  
499 attempted in a few regions. This is due to leakage of the much larger mass fluctuations from  
500 land hydrology and cryosphere variability into the ocean (Wahr et al., 1998), particularly  
501 important at seasonal and longer time scales. Land (and ice sheet) mass variability is often one  
502 to two orders of magnitude larger than ocean mass variations, and it is difficult to estimate the  
503 leaked signal without knowing the signal that is being leaked. Some studies have attempted to  
504 correct for the leakage by iterating with GRACE estimates of land and ice sheet mass changes  
505 (Chambers and Bonin, 2012), using an inverse method where land and ocean signals are  
506 separated by pre-defined basins (Chen et al., 2013), or, more recently, using a predefined mesh  
507 of global mass concentrations, or mascons, to separate ocean and land signals (e.g., Lemoine  
508 et al., 2007; Watkins et al., 2015; Save et al., 2016).

509 There have been a few studies where GRACE data in coastal waters have been utilized and  
510 shown to explain a large percentage of sea level variance in coastal waters. Landerer et al.  
511 (2015) used a GRACE mascon solution to study variability in the Atlantic Meridional  
512 Overturning Circulation (AMOC). This required using GRACE-derived ocean bottom pressure  
513 along the United States eastern continental shelf, within 300 km of land. Although they could  
514 resolve interannual fluctuations in the bottom pressure associated with changes in the AMOC,  
515 they found a large, unrealistic trend that they speculated had to be from residual leakage of  
516 hydrology signals, even using a mascon solution. GRACE has also shown some level of  
517 accuracy in measuring coastal level in two small enclosed gulfs with large sea level variability  
518 that is caused by winds at annual periods: the Gulf of Carpentaria in northern Australia  
519 (Tregoning et al., 2008) and the Gulf of Thailand (Wouters and Chambers, 2010).

520 Newer mascon solutions from GRACE show more promise of being able to recover the ocean  
521 mass (barotropic) portion of sea level variability in substantially more coastal waters. Piecuch  
522 et al. (2018b) compared ocean bottom pressure from a GRACE mascon solution from the Jet  
523 Propulsion Laboratory that incorporated a special filter to optimally separate land and ocean  
524 signals (Watkins et al., 2015; Wiese et al., 2016). They found that these new GRACE mascon  
525 solutions explained ~30-50% of the sea level variance measured by tide gauges along the  
526 Australian shelf, the North Sea around Scandinavia, the eastern coast of the United States and  
527 Canada, and around parts of the Chinese coast and Indonesian archipelago. While much of this  
528 correspondence is due to the annual signal, Piecuch et al. (2018b) do demonstrate good  
529 agreement with interannual and non-seasonal sea level and ocean bottom pressure in many of  
530 these same areas. This is expected from theory, since in shallower waters there should be a  
531 greater coupling between sea level and ocean bottom pressure as the response will be more  
532 barotropic. Thus, although GRACE data have not regularly been used to understand coastal sea  
533 level variability, new processing has improved the accuracy sufficiently that the satellite ocean  
534 bottom pressure can be useful in understanding coastal sea level variability in shallow waters  
535 with a wide shelf.

536 Another area where GRACE has demonstrated usefulness is in measuring a portion of coastal  
537 sea level that results from gravitational changes due to land ice melting (e.g., Riva et al., 2010)  
538 and fluctuations in land hydrology (e.g., Jensen et al., 2013). Although important for

539 understanding and predicting sea level rise a hundred years from now, these are minor signals  
540 in coastal sea level measurements made by tide gauges.

## 541 **6. Steric sea-level observations**

542 Knowledge about hydrographic changes (from temperature and salinity) is crucial for  
543 interpreting sea-level variability and underlying mechanisms, especially in the open ocean, but  
544 with impact also along the coastal zones. This section offers a summary of existing observing  
545 capabilities of the most relevant variables and discusses improvements on coverage, integration  
546 and other issues that could be helpful over the next decade.

547 Knowledge of temperature (T) and salinity (S) distributions can provide information on steric  
548 contributions to coastal sea-level variability. As they relate to density, T and S data also carry  
549 dynamic information (pressure gradients, velocities). Combined with bottom pressure and  
550 other variables, T and S data can be used to elucidate many aspects of sea-level behaviour (e.g.,  
551 separating oceanographic and geodetic contributions, discerning causal and forcing  
552 mechanisms).

553 With Argo floats not sampling the shallow regions, there are no operational global in-situ  
554 observations of coastal T and S, but regional efforts have been implemented over the years  
555 using both ship-based and moored platforms (e.g., data collection in many coastal regions set  
556 up under the U.S. Integrated Ocean Observing System; <https://ioos.noaa.gov/regions/>) and  
557 more recently glider technology (e.g., <https://gliders.ioos.us/>; Pattiaratchi et al. 2017; Rudnick  
558 et al. 2017; Heslop et al. 2012). One challenge and perhaps a worthy long-term focus will be  
559 to link available T and S data to sea level data at the local level, particularly as coastal observing  
560 systems attain operational status.

561 In the case of surface measurements, satellite retrievals provide a useful, global alternative to  
562 in-situ platforms, albeit at varying resolutions and with questionable accuracy near the coastal  
563 zone, mostly due to the fact most of the in-situ platforms for calibration/validation are offshore  
564 (Brewin et al., 2017). For sea surface temperature (SST), a variety of remotely sensed and  
565 blended products exist at typical daily sampling, nominal kilometre resolutions, and accuracies  
566 of ~0.5K (Donlon et al. 2007, 2009; <https://www.ghrsst.org/>). Although SST has been shown  
567 to correlate with sea level over deep water (Meyssignac et al., 2017), the case for the coastal  
568 ocean remains to be explored. To the extent that SST can reflect steric sea level, high resolution  
569 satellite products could be used to infer potential short scale structures affecting sea level across  
570 the coastal zone. Such knowledge can, for example, inform comparisons of tide gauge and  
571 altimeter sea level data, which are affected by their different spatial sampling characteristics.

572 Sea surface salinity (SSS) retrievals are much more recent and not as mature nor operational  
573 as SST. The Aquarius mission lasted over the period 2011-2015, but the Soil Moisture Ocean  
574 Salinity (SMOS) mission continues to be operational since 2009, and data from the Soil  
575 Moisture Active Passive (SMAP) mission launched in 2015 has also become available (e.g.,  
576 Mecklenburg et al. 2016; Weissman et al. 2017; Köhler et al. 2018; Boutin et al. 2018).  
577 Nominal sampling ranges from weekly to monthly at resolutions of ¼ to 1 degree (around 40  
578 km for SMAP), and with typical accuracies of ~0.2 psu. Apart from the challenges of relating  
579 SSS retrievals to bulk and to subsurface S (e.g., Boutin et al., 2018), the extent to which these  
580 quantities are related to coastal sea level has not been explored in any detail. Sea level and SSS  
581 are expected to be linked directly through the effects of river runoff (Meade and Emery 1971),  
582 but the related SSS signals can be trapped to the coast on scales that are not well resolved with  
583 the currently available satellite systems (Durand et al., 2018; Picuch et al., 2018a). Similar  
584 issues may also affect the ability to observe possible impacts of ice melt on coastal sea level at  
585 high latitudes.

## 586 7. Discussion and final remarks

587 Monitoring networks of in-situ coastal sea level are presently well developed along most of the  
588 world coastlines, although with notable exceptions in Africa and part of South America, where  
589 the spatial density of instruments is significantly lower than, for example, in Europe.  
590 Furthermore, delayed-mode, low-frequency tide gauge data in some parts of the coastlines  
591 (including the above-mentioned regions but also others like the Arctic Ocean) are not routinely  
592 released to the international databases, limiting the available information in these areas even  
593 more. The same geographical bias applies to high-frequency sea-level measurements, as these  
594 come from the same tide gauges.

595 The lack of sea level information on poorly sampled regions may be partly overcome with  
596 coastal altimetry observations. Despite the longer revisit time of the altimeters, there is a clear  
597 complementarity between tide gauges and altimetry that should be exploited in order to  
598 improve the current knowledge of sea level variations in coastal regions at low frequencies  
599 (monthly and longer periods). In this respect, the information on VLM at the tide gauge is  
600 crucial for the consistency between both measurements. This is achieved through GNSS  
601 observations and can be further complemented with other geodetic techniques, such as InSAR  
602 to extend VLM estimates to larger areas. In the near future, progress in data processing and the  
603 continuity of altimetric missions are promising for coastal sea-level studies. This includes the  
604 forthcoming SWOT mission (Durand et al., 2010) and the already operational Sentinel  
605 missions from the European Space Agency (<https://sentinel.esa.int/web/sentinel/missions>).

606 Overall, an integrated coastal sea-level observing system should:

- 607 1) be able to accurately measure sea-level changes at the coast itself at high frequency  
608 rates (hourly or higher, to account for extreme sea levels) and at the nearby coastal  
609 region, using in-situ (tide gauges) and satellite altimetry observations, respectively;
- 610 2) use GNSS observations to provide information on VLM in order to separate ocean and  
611 land signals in in-situ measurements, especially in the long-term when both components  
612 can be of the same order of magnitude;
- 613 3) measure local and regional sea-level contributors, including offshore and coastal wind-  
614 waves, water density changes, surface meteorological parameters (atmospheric  
615 pressure and winds being among the most important; see Piecuch et al, this issue), and  
616 in general any other local process important to identify and understand the coastal  
617 dynamics inducing sea-level variations (e.g. river run-off, Durand et al, this issue);
- 618 4) be consolidated on a long-term basis.

619 The scientific and societal benefits of such a system are numerous. Climate studies require  
620 long-term, consistent and continuous measurements. In this respect, consolidation of observing  
621 systems is crucial to avoid endangering the continuity of the observations and introducing data  
622 gaps. Currently, this is ensured for satellite missions (altimetry and gravimetry) but,  
623 unfortunately, even in intensively monitored regions, like Europe, national agencies have  
624 reported problems with securing funding for maintenance of the current tide gauge networks  
625 (Pérez et al, 2017), representing a serious concern especially for the valuable long-term records.  
626 An integrated observing system of sea-level and related variables would also provide consistent  
627 information to be assimilated into numerical models, including the quantification of data  
628 uncertainties that are critical in analyses and model forecasts. It would further contribute to  
629 operational oceanographic systems and warning protocols (e.g. flood warnings). Finally, it is  
630 also an adequate framework to foster technological development of new emerging monitoring  
631 platforms capable of expanding current in-situ observations (e.g. GNSS-towed platforms) and  
632 thus contributing to maximise the information provided by in-situ sea-level measurements.

633 Observing sea-level changes at the coast and quantifying its drivers is the first step to  
634 understand the complex dynamics of the coastal region, to link the responses of the coastal  
635 environment to sea-level changes and to anticipate how projected sea-level variations will  
636 impact the coastal areas.

637

## 638 References

639 André BG, Martín Míguez B, Ballu V, et al (2013) Measuring sea level with GPS-equipped  
640 buoys: a multi-instruments experiment at Aix Island. *Int Hydrographic Rev* 27–38

641 Ardhuin F, Drake T G, Herbers T H C (2002) Observations of wave-generated vortex ripples  
642 on the North Carolina continental shelf. *J Geophys Res* 107 C10. doi:10.1029/2001JC000986.

643 Ardhuin F, Devaux E, Pineau-Guillou L (2010) Observation et prévision des seiches sur la côte  
644 atlantique française. Actes des Xèmes journées Génie côtier-Génie civil, Les Sables d’Olonne,  
645 87–94, Centre Français du Littoral, doi:10.5150/jngcgc.2010.001-A.

646 Ardhuin F, Rasclé N, Chapron B, Gula J, Molemaker J, Gille S T, Menemenlis D, Rocha C  
647 (2017) Small scale currents have large effects on wind wave heights. *J Geophys Res* 122 C6  
648 4500–4517. doi:10.1002/2016JC012413.

649 Ardhuin F, Aksenov Y, Benetazzo A, Bertino L, Brandt P, Caubet E, Chapron B, Collard F,  
650 Cravatte S, Dias F, Dibarboure G, Gaultier L, Johannessen J, Korosov A, Manucharyan G,  
651 Menemenlis D, Menendez M, Monnier G, Mouche A, Nougier F, Nurser G, Rampal P,  
652 Reniers A, Rodriguez E, Stopa J, Tison C, Tissier M, Ubelmann C, van Sebille E, Vialard J,  
653 Xie J (2018) Measuring currents, ice drift, and waves from space: the sea surface kinematics  
654 multiscale monitoring (SKIM) concept. *Ocean Sci* 14: 337–354. doi:10.5194/os-2017-65.

655 Ballu V, Bouin M-N, Calmant S, et al (2010) Absolute seafloor vertical positioning using  
656 combined pressure gauge and kinematic GPS data. *J Geod* 84:. doi: 10.1007/s00190-009-0345-  
657 y

658 Ballu V, Testut L, Poirier E, et al (2017) Mapping the sealevel for altimetry calibration purpose  
659 using the future PAMELi marine ASV around the Aix Island sea-level observatory. In: 2017  
660 Ocean Surface Topography Science Team Meeting. Miami

661 Battjes J A (1982) A case study of wave height variations due to currents in a tidal entrance.  
662 *Coastal Eng* 6:47–57.

663 Bergmann I, Dobsław H (2012) Short-term transport variability of the Antarctic Circumpolar  
664 Current from satellite gravity observations. *J. Geophys. Res.* 117 (C05044).  
665 doi:10.1029/2012JC007872.

666 Bertin X, de Bakker A, van Dongeren A, Coco G, Andre G, Ardhuin F, Bonneton P, Bouchette  
667 F, Castelle B, Crawford W, Deen M, Dodet G, Guerin T, Leckler F, McCall R, Muller H,  
668 Olabarrieta M, Ruessink G, Sous D, Stutzmann E, Tissier M (2018) Infragravity waves: from  
669 driving mechanisms to impacts. *Earth-Science Rev* 177:774–799.  
670 doi:10.1016/j.earscirev.2018.01.002.

671 Birol F, Fuller N, Lyard F, Cancet M, Niño F, Delebecque C, Fleury S, Toub Blanc F, Melet A,  
672 Saraceno M, Leger F (2016) Coastal applications from nadir altimetry: example of the X-  
673 TRACK regional products. *Advances in Space Research*. doi:10.1016/j.asr.2016.11.005.

674 Boening C, Willis J K, Landerer F W, Nerem R S, Fasullo J (2012) The 2011 La Niña: So  
675 strong, the oceans fell. *Geophys. Res. Lett.* 39 (L19602). doi:10.1029/2012GL053055.

676 Bonnefond P, Exertier P, Laurain O, et al (2003a) Absolute Calibration of Jason-1 and  
677 TOPEX/Poseidon Altimeters in Corsica Special Issue: Jason-1 Calibration/Validation. *Mar*  
678 *Geod* 26:261–284. doi: 10.1080/714044521

679 Bonnefond P, Exertier P, Laurain O, et al (2003b) Leveling the Sea Surface Using a GPS-  
680 Catamaran Special Issue: Jason-1 Calibration/Validation. *Mar Geod* 26:319–334. doi:  
681 10.1080/714044524

682 Boutin J, Vergely JL, Marchand S, D'Amico F, Hasson A, Kolodziejczyk N, Reul N, Reverdin  
683 G, Vialard J (2018) New SMOS Sea Surface Salinity with reduced systematic errors and  
684 improved variability. *Remote Sensing of Environment*, 214:115-134,  
685 <https://doi.org/10.1016/j.rse.2018.05.022>.

686 Born GH, Michael PE, Axelrad P, et al (1994) Calibration of the TOPEX altimeter using a GPS  
687 buoy. *J Geophys Res Ocean* 99:24517–24526. doi: 10.1029/94JC00920

688 Bouin M-N, Ballu V, Calmant S, et al (2009a) A kinematic GPS methodology for sea surface  
689 mapping, Vanuatu. *J Geod* 83:. doi: 10.1007/s00190-009-0338-x

690 Bouin M-N, Ballu V, Calmant S, Pelletier B (2009b) Improving resolution and accuracy of  
691 mean sea surface from kinematic GPS, Vanuatu subduction zone. *J Geod* 83:. doi:  
692 10.1007/s00190-009-0320-7

693 Boutin J, Chao Y, Asher WE, Delcroix T, Drucker R, Drushka K, Kolodziejczyk N, Lee T,  
694 Reul N, Reverdin G, Schanze J, Soloviev A, Yu L, Anderson J, Brucker L, Dinnat E, Santos-  
695 Garcia A, Jones WL, Maes C, Meissner T, Tang W, Vinogradova N, Ward B (2016) Satellite  
696 and In Situ Salinity: Understanding Near-Surface Stratification and Subfootprint Variability.  
697 *Bull. Amer. Meteor. Soc.*, 97:1391–1407, <https://doi.org/10.1175/BAMS-D-15-00032.1>.

698 Bradshaw E, Rickards L, Aarup T (2015) Sea level data archaeology and the Global Sea Level  
699 Observing System(GLOSS). *Geo Res J* 6:9–16. 10.1016/j.grj.2015.02.005

700 Brewin RJW, de Mora L, Billson O, Jackson T, Russell P, Brewin TG, Shutler JD, Miller PI,  
701 Taylor BH, Smyth TJ, Fishwick JR (2017) Evaluating operational AVHRR sea surface  
702 temperature data at the coastline using surfers. *Estuarine, Coastal and Shelf Science* 196:276-  
703 289, ISSN 0272-7714, <https://doi.org/10.1016/j.ecss.2017.07.011>

704 Calafat FM, Wahl T, Lindsten F, Williams J, Frajka-Williams E (2018) Coherent modulation  
705 of the sea-level annual cycle in the United States by Atlantic Rossby waves. *Nature*  
706 *Communications* 9:2571. 10.1038/s41467-018-04898-y

707 Calzas M, Brachet C, Drezen C, et al (2014) New technological development for cal/val  
708 activities. In: 2014 Ocean Surface Topography Science Team Meeting. Lake Constance,  
709 Germany

710 Cariolet J-M, Suanez S (2013) Runup estimations on a macrotidal sandy beach. *Coast Eng*  
711 74:11–18.

712 Cartwright D E (1977) Oceanic Tides. *Rep Prog Phys* 40: 665-708.

713 Chambers D P, Wahr J, Nerem R S (2004) Preliminary observations of global ocean mass  
714 variations with GRACE. *Geophys Res Lett* 31:L13310. doi:10.1029/2004GL020461.

715 Chambers D P, Bonin J A (2012) Evaluation of Release-05 GRACE time-variable gravity  
716 coefficients over the ocean. *Ocean Science* 8:1–10. DOI:10.5194/os-8-1-2012.

717 Chambers D P, Cazenave A, Champollion N, Dieng H, Llovel W, Forsberg R, von Schuckmann  
718 K, Wada Y (2017) Evaluation of the Global Mean Sea Level Budget between 1993 and 2014.  
719 *Surv Geophys* 38:309-327. doi: 10.1007/s10712-016-9381-3.

720 Chen J L, Wilson C R, Tapley B D (2013) Contribution of ice sheet and mountain glacier melt  
721 to recent sea level rise. *Nature Geoscience* 6:549-552. DOI: 10.1038/NGEO1829.

722 Church J A, Clark P U, Cazenave A, Gregory J M, Jevrejeva S, Levermann A, Merrifield M  
723 A, Milne G A, Nerem R S, Nunn P D, Payne A J, Pfeffer W T, Stammer D, Unnikrishnan A S  
724 (2013) Sea level change, in: *Climate Change 2013: The Physical Science Basis. Contribution*  
725 *of Working Group I to the Fifth Assessment Report of the Intergovernmental Panel on Climate*  
726 *Change*. Edited by: Stocker T F, Qin D, Plattner G-K, Tignor M, Allen S K, Boschung J, Nauels  
727 A, Xia Y, Bex V, and Midgley P M. Cambridge University Press, Cambridge, UK and New  
728 York, NY, USA.

729 Cipollini P, Calafat F M, Jevrejeva S, Melet S, Prandi P (2017) Monitoring sea level in the  
730 coastal zone with satellite altimetry and tide gauges. *Surveys in Geophysics* 38(1): 33-57. doi:  
731 [10.1007/s10712-016-9392-0](https://doi.org/10.1007/s10712-016-9392-0).

732 Coco G, Senechal N, Rejas A, Bryan K R , Capo S, Parisot J P , Brown J A , MacMahan, J H  
733 M (2014) Beach response to a sequence of extreme storms. *Geomorphology* 204:493-501.

734 Coulombier T, Ballu V, Pineau P, et al (2018) PAMELi, un drone marin de surface au service  
735 de l'interdisciplinarité. *Paralia* 15:337–344. doi: DOI:10.5150/jngcgc.2018.038

736 Dangendorf S, Marcos M, Woppelmann G, Conrad CP, Frederikse T, Riva R (2017)  
737 Reassessment of 20th century global mean sea level rise. *PNAS* 114, doi:  
738 10.1073/pnas.1616007114

739 Dodet G, Melet A, Ardhuin F, Almar R, Bertin X, Idier D, Pedredos R (submitted) The  
740 Contribution of Wind Generated Waves to Coastal Sea Level Changes. *Surveys in Geophysics*

741 Donlon C, Rayner N, Robinson I, Poulter DJS, Casey KS, Vazquez-Cuervo J, Armstrong E,  
742 Bingham A, Arino O, Gentemann C, et al. (2007) The global ocean data assimilation  
743 experiment high-resolution sea surface temperature pilot project. *Bull. Am. Meteorol. Soc.*,  
744 88:1197–1213.

745 Donlon CJ, Casey KS, Robinson IS, Gentemann CL, Reynolds RW, Barton I, Arino O, Stark  
746 J, Rayner N, LeBorgne P, Poulter D, Vazquez-Cuervo J, Armstrong E, Beggs H, Llewellyn-  
747 Jones D, Minnett PJ, Merchant CJ, Evans R (2009) GODAE High-Resolution Sea Surface  
748 Temperature Pilot Project. *Oceanography* 22(3):34–45, doi:10.5670/oceanog.2009.64.

749 Dugan J P, Morris W D, Vierra K C, Piotrowski C C, Farruggia G J, Campion D C (2001)  
750 Jetski-based nearshore bathymetric and current survey system. *Journal of coastal research* 900-  
751 908.

752 Durand M, Fu L-L, Lettenmaier DP, Alsdorf DE, Rodriguez E, Esteban-Fernandez D (2010)  
753 The Surface Water and Ocean Topography Mission: Observing Terrestrial Surface Water and  
754 Oceanic Submesoscale Eddies. *Proceedings of the IEEE* 98, doi:  
755 10.1109/JPROC.2010.2043031

756 Durand F, Calmant S, Calzas M, et al (2017) Geodetic survey of the freshwater front of the  
757 Ganges-Brahmaputra freshwater plume in the northern Bay of Bengal from Calnago GNSS  
758 device. In: 2017 Ocean Surface Topography Science Team Meeting

759 Durand F, Piecuch C, Cirano M, Becker M, Papa F (submitted) Runoff impact on coastal sea  
760 level. *Surveys in Geophysics*.

761 Fantino M, Marucco G, Mulassano P, Pini M (2008) Performance analysis of MBOC, AltBOC  
762 and BOC modulations in terms of multipath effects on the carrier tracking loop within GNSS  
763 receivers. *IEEE/ION Position, Location and Navigation Symposium* DOI:  
764 10.1109/PLANS.2008.4570092

765 Fasullo J T, Boening C, Landerer F W, Nerem R S (2013) Australia's unique influence on  
766 global sea level in 2010–2011. *Geophys. Res. Lett.* 40:4368–4373. doi:10.1002/grl.50834.

767 Foster J H, Carter G S, Merrifield M A (2009) Ship-based measurements of sea surface  
768 topography. *Geophysical Research Letters* 36: L11605.  
769 <https://doi.org/10.1029/2009GL038324>

770 Fund F, Perosanz F, Testut L, Loyer S (2013) An Integer Precise Point Positioning technique  
771 for sea surface observations using a GPS buoy. *Adv Sp Res* 51:1311–1322. doi:  
772 10.1016/j.asr.2012.09.028

773 Gemmrich J, Thomas B, Bouchard R (2011) Observational changes and trends in northeast  
774 Pacific wave records *Geophys Res Lett* 38:L22601. doi:10.1029/2011GL049518.

775 Haines B, Desai S, Dodge A, et al (2017) Connecting Jason-3 to the long-term sea level record:  
776 results from harvest and regional campaigns. In: 2017 Ocean Surface Topography Science  
777 Team Meeting

778 Hauser D, Tison C, Amiot T, Delaye L, Corcoral N, Castillan P (2017) SWIM: The first  
779 spaceborne wave scatterometer. *IEEE Trans. on Geosci. and Remote Sensing*, 55, 5:3000–  
780 3014.

781 Hein GW, Landau H, Blomenhofer H (1990) Determination of instantaneous sea surface, wave  
782 heights, and ocean currents using satellite observations of the global positioning system. *Mar*  
783 *Geod* 14:217–224. doi: 10.1080/15210609009379664

784 Heslop EE, Ruiz S, Allen J, LópezUnitez-Jurado JL, Renault L, Tintoré J (2012) Autonomous  
785 underwater gliders monitoring variability at “choke points” in our ocean system: A case study  
786 in the Western Mediterranean Sea. *Geophys. Res. Lett.*, 39, doi:10.1029/2012GL053717

787 Hogarth P (2014) Preliminary analysis of acceleration of sea level rise through the twentieth  
788 century using extended tide gauge data sets (August 2014). *J Geophys Res Oceans* 119:7645–  
789 7659. 10.1002/2014JC009976.

790 Holgate S J, Matthews A, Woodworth PL, Rickards LJ, Tamisiea ME, Bradshaw E, Foden PR,  
791 Gordon KM, Jevrejeva S, Pugh J (2013) New data systems and products at the Permanent  
792 Service for Mean Sea Level. *J Coast Res* 29:493–504.

793 Holman R, Plant N, Holland T (2013) cBathy: A robust algorithm for estimating nearshore  
794 bathymetry. *Journal of Geophysical Research: Oceans* 118(5):2595-2609.

795 Hughes C W, Tamisiea M E, Bingham R J, Williams J (2012) Weighing the ocean: Using a  
796 single mooring to measure changes in the mass of the ocean. *Geophysical Research Letters*,  
797 39, L17602, doi:10.1029/2012GL052935

798 Intergovernmental Oceanographic Commission (IOC) (1985) Manual on Sea Level  
799 Measurement and Interpretation (Volume I—Basic Procedures). Intergov. Oceanogr. Comm.  
800 Manuals and Guides, 14, UNESCO, Paris. [Available at  
801 [http://www.psmsl.org/train\\_and\\_info/training/manuals/ioc\\_14i.pdf.](http://www.psmsl.org/train_and_info/training/manuals/ioc_14i.pdf)]

802 Jensen L, Rietbroek R, Kusche J (2013) Land water contribution to sea level from GRACE and  
803 Jason-1 measurements. *J. Geophys. Res. Oceans* 118:212–226. doi:10.1002/jgrc.20058

804 Johnson G F, Chambers D P (2013) Ocean Bottom Pressure Seasonal Cycles and Decadal  
805 Trends from GRACE Release-05: Ocean Circulation Implications. *J. Geophys. Res. Oceans*  
806 118:1-13. doi:10.1002/jgrc.20307.

807 Köhler J, Serra N, Bryan FO, Johnson BK, Stammer D (2018) Mechanisms of mixed-layer  
808 salinity seasonal variability in the Indian Ocean, *Journal of Geophysical Research: Oceans*,  
809 123:466–496, <https://doi.org/10.1002/2017JC013640>.

810 Landerer F W, Wiese D N, Bentel K, Boening C, Watkins M M (2015) North Atlantic  
811 meridional overturning circulation variations from GRACE ocean bottom pressure anomalies.  
812 *Geophys. Res. Lett.* 42. doi:10.1002/2015GL065730.

813 Larson KM, Ray RD, Nievinski FG, Freymueller JT (2013) The Accidental Tide Gauge: A  
814 GPS Reflection Case Study From Kachemak Bay, Alaska. *IEEE Geoscience and remote  
815 sensing letters* 10

816 Laurichesse D, Mercier F, Berthias J-P, et al (2009) Integer Ambiguity Resolution on  
817 Undifferenced GPS Phase Measurements and Its Application to PPP and Satellite Precise Orbit  
818 Determination. *Navigation* 56:135–149. doi: 10.1002/j.2161-4296.2009.tb01750.x

819 Lemoine FG, Luthcke S B, Rowlands D D, Chinn D S, Klosko S M, Cox C M (2007) The use  
820 of mascons to resolve time-variable gravity from GRACE, in *Dynamic Planet: Monitoring and  
821 Understanding a Dynamic Planet with Geodetic and Oceanographic Tools*. Edited by:  
822 Tregoning P, Rizos C. *Intl. Assoc. of Geodesy Symposia*, Springer, Berlin 130:231-236.

823 Leuliette E W, Miller L (2009) Closing the sea level rise budget with altimetry, Argo, and  
824 GRACE. *Geophys. Res. Lett.* 36:L04608. doi:10.1029/2008GL036010.

825 Lowe R J, Falte, J L, Koseff J R, Monismith S G, Atkinson M J (2007) Spectral wave flow  
826 attenuation within submerged canopies: Implications for wave energy dissipation. *J. Geophys.  
827 Res.* 112, doi:10.1029/2006JC003605.

828 Magne R, Belibassakis K, Herbers T H C, Arduin F, O'Reilly W C, Rey V (2007) Evolution  
829 of surface gravity waves over a submarine canyon, *J. Geophys. Res.* 112  
830 doi:10.1029/2005JC003035.

831 Makowski J K, Chambers D P, and Bonin J A (2015) Using Ocean Bottom Pressure from the  
832 Gravity Recovery and Climate Experiment (GRACE) to Estimate Transport Variability in the  
833 Southern Indian Ocean. *J. Geophys. Res. Oceans* 120. doi: 10.1002/2014JC010575

834 Marcos M, Puyol B, Wöppelmann G, Herrero C, García-Fernández MJ (2011) The long sea  
835 level record at Cadiz (southern Spain) from 1880 to 2009. *J Geophys Res* 116:C12003.  
836 10.1029/2011JC007558.

837 Martín Míguez B, Le Roy R, Wöppelmann G (2008) The Use of Radar Tide Gauges to Measure  
838 Variations in Sea Level along the French Coast. *Journal of Coastal Research* 24:61 – 68.

839 Martín Míguez B, Testut L, Wöppelmann G (2012) Performance of modern tide gauges:  
840 Towards mm-level accuracy. *Sci Mar* 76:221–228. doi: DOI: 10.3989/scimar.03618.18A

841 Mastenbroek, C., Burgers, G., and Janssen, P. A. E. M. (1993) The dynamical coupling of a  
842 wave model and a storm surge model through the atmospheric boundary layer, *J. Phys.  
843 Oceanogr.*, 23, 1856–1867.

844 Masselink G, Scott T, Poate T, Russell P, Davidson M, Conley D (2016) The extreme  
845 2013/2014 winter storms: hydrodynamic forcing and coastal response along the southwest  
846 coast of England. *Earth Surface Processes and Landforms*, 41(3):378-391.

847 Meade RH, Emery KO (1971) Sea Level as Affected by River Runoff, Eastern United States.  
848 *Science* 173(3995):425–428.

849 Mecklenburg S, Drusch M, Kaleschke L, Rodriguez-Fernandez N, Reul N, Kerr Y, Font J,  
850 Martin-Neira M, Oliva R, Daganzo-Eusebio E, Grant JP, Sabia R, Macelloni G, Rautiainen K,  
851 Fauste J, de Rosnay P, Munoz-Sabater J, Verhoest N, Lievens H, Delwart S, Crapolicchio R,  
852 de la Fuente A, Kornberg M (2016) ESA's Soil Moisture and Ocean Salinity mission: From  
853 science to operational applications. *Remote Sensing of Environment*, 180:3-18,  
854 <https://doi.org/10.1016/j.rse.2015.12.025>.

855 Meinig C, Stalin S E, Nakamura A I, Milburn H B (2005) Real-Time Deep-Ocean Tsunami  
856 Measuring, Monitoring, and Reporting System: The NOAA DART II Description and  
857 Disclosure. NOAA, Pacific Marine Environmental Laboratory (PMEL), 1-15.

858 Meyssignac B, Piecuch CG, Merchant CJ, Racault, M-F, Palanisamy H, MacIntosh C,  
859 Sathyendranath S, Brewin R (2017) Causes of the regional variability in observed sea level,  
860 sea surface temperature and ocean color over the period 1993-2011. *Surv. Geophys.*, 38:187-  
861 215, <https://doi.org/10.1007/s10712-016-9383-1>.

862 Munk W H, Traylor M A (1947) Refraction of ocean waves: a process linking underwater  
863 topography to beach erosion. *Journal of Geology*, LV 1–26.

864 Okihiro M, Guza R T, Seymour R J (1993) Excitation of seiche observed in a small harbor, *J.*  
865 *Geophys. Res.* 98 C10:18201–18211

866 Pattiaratchi C, Woo LM, Thomson PG, Hong KK, Stanley D (2017) Ocean glider observations  
867 around Australia. *Oceanography*, 30(2):90–91, <https://doi.org/10.5670/oceanog.2017.226>.

868 Penna NT, Morales Maqueda MA, Martin I, et al (2018) Sea Surface Height Measurement  
869 Using a GNSS Wave Glider. *Geophys Res Lett* 45:5609–5616. doi: 10.1029/2018GL077950

870 Pérez Gómez B, Donato V, Hibbert A, Marcos M, Raicich F, Hammarklint T, Testut L,  
871 Annunziato A, Westbrook G, Gyldenfeldt A, Goringe (2017) Recent Efforts for an Increased  
872 Coordination of Sea Level Monitoring in Europe: EuroGOOS Tide Gauge Task Team.  
873 International WCRP/IOC Conference 2017: Regional Sea Level Changes and Costal Impacts,  
874 New York 2017

875 Piecuch C G, Quinn K J, Ponte R M (2013) Satellite-derived interannual ocean bottom pressure  
876 variability and its relation to sea level. *Geophys. Res. Lett.* 40. doi:10.1002/grl.50549.  
877

878 Piecuch CG, Bitterman K, Kemp AC, Ponte RM, Little CM, Engelhart SE, Lentz SJ (2018a)  
879 River-discharge effects on United States Atlantic and Gulf coast sea-level changes. *Proc.Nat.*  
880 *Acad. Sci.*, Jul 2018, 201805428; DOI: 10.1073/pnas.1805428115.

881 Piecuch C G, Landerer F W, Ponte R M (2018b) Tide gauge records reveal improved  
882 processing of gravity recovery and climate experiment time-variable mass solutions over the  
883 coastal ocean, *Geophysical Journal International*, 214, 1401–1412,  
884 <https://doi.org/10.1093/gji/ggy207>.

885 Pineau-Guillou L, Arduin F, Bouin M-N, Redelsperger J-L, Chapron B, Bidlot J, Quilfen Y  
886 (2018) Strong winds in a coupled wave-atmosphere model during a north atlantic storm event:

887 evaluation against observations. *Quart. Journ. Roy. Meteorol. Soc.*, 144:317–332.  
888 doi:10.1002/qj.3205.

889 Polster A, Fabian M, Villinger H (2009) Effective resolution and drift of Paroscientific pressure  
890 sensors derived from longterm seafloor measurements. *Geochem. Geophys. Geosyst.* 10,  
891 Q08008, doi:10.1029/2009GC002532

892 Ponte R M, Piecuch C G (2014) Interannual Bottom Pressure Signals in the Australian–  
893 Antarctic and Bellingshausen Basins. *J. Phys. Ocean.* 44:1456-1465. DOI: 10.1175/JPO-D-13-  
894 0223.1

895 Pugh D, Woodworth PL (2014) *Sea-Level Science: Understanding Tides, Surges, Tsunamis  
896 and Mean Sea-Level Changes.* Cambridge University Press, Online ISBN: 9781139235778  
897 <https://doi.org/10.1017/CBO9781139235778>

898 Raubenheimer, B. (2002). Observations and predictions of fluid velocities in the surf and swash  
899 zones. *Journal of Geophysical Research: Oceans*, 107(C11), 11-1.

900 Ray, R. D., (2013). Precise comparisons of bottom-pressure and altimetric ocean tides. *J.*  
901 *Geophys.*

902 Reinking J, Härting A, Bastos L (2012) Determination of sea surface height from moving ships  
903 with dynamic corrections. *Journal of Geodetic Science* 2:172–187.  
904 <https://doi.org/10.2478/v10156-011-0038-3>

905 Rietbroek R, Brunnabend S E, Kusche J, Schröter J, Dahle C (2016) Revisiting the  
906 contemporary sea-level budget on global and regional scales. *Proc. Natl. Acad. Sci.* 113:1504-  
907 1509. doi: 10.1073/pnas.1519132113.

908 Riva R E M, Bamber J L, Lavallée D A, Wouters B (2010), Sea-level fingerprint of continental  
909 water and ice mass change from GRACE. *Geophys. Res. Lett.* 37:L19605.  
910 doi:10.1029/2010GL044770.

911 Rocken C, Kelecy TM, Born GH, et al (1990) Measuring precise sea level from a buoy using  
912 the global positioning system. *Geophys Res Lett* 17:2145–2148. doi:  
913 10.1029/GL017i012p02145

914 Rudnick DL, Zaba KD, Todd RE, Davis RE (2017) A climatology of the California Current  
915 System from a network of underwater gliders. *Progress in Oceanography*, 154:64-106,  
916 <https://doi.org/10.1016/j.pocean.2017.03.002>

917  
918 Santamaría-Gómez A, Watson C (2017). Remote leveling of tide gauges using GNSS  
919 reflectometry: case study at Spring Bay, Australia *GPS Solut*, 21(2), DOI 10.1007/s10291-  
920 016-0537-x

921  
922 Santamaría-Gómez A, Gravelle M, Dangendorf S, Marcos M, Spada G, Wöppelmann G  
923 (2017). Uncertainty of the 20th century sea-level rise due to vertical land motion errors. *Earth  
924 and Planetary Science Letters* 473, 24–32

925 Sasagawa G, Cook MJ, Zumberge MA (2016). Drift-corrected seafloor pressure observations  
926 of vertical deformation at Axial Seamount 2013–2014. *Earth and Space Science* 3 381–385,  
927 doi:10.1002/2016EA000190.

928 Save H, Bettadpur S, Tapley B D (2016) High resolution CSR GRACE RL05 mascons. *J.*  
929 *Geophys. Res. Solid Earth* 121:7547–7569. doi:10.1002/2016JB013007.

930 Senechal N, Abadie S, Ardhuin F, Bujan S, Capo S, Certain R, Coco G, Gallagher E, Garlan  
931 T, Masselink G, MacMahan J, Michallet H, Pedreros R, Reniers A, Rey V, Ruessink B, Russell  
932 P, Turner I (2011a) The ECORS-Truc Vert 2008 field experiment: extreme storm conditions  
933 over a three-dimensional morphology system in a macro-tidal environment. *Ocean Dynamics*  
934 61:2073–2098, doi:10.1007/s10236-011-0472-x.

935 Senechal, N., Coco, G., Bryan, K.R., Holman, R.A., 2011b, Wave runup during extreme storm  
936 conditions, *Journal of Geophysical Research*, 116, C07032, doi:10.1029/2010JC006819.

937 Spencer R, Foden P R, McGarry C, Harrison A J, Vassie J M, Baker T F, Smithson M J,  
938 Harangozo S A, Woodworth P L (1993) The ACCLAIM programme in the South Atlantic and  
939 southern oceans. *International Hydrographic Review* 70 (1):7-21.

940 Stephens S, Coco G, Bryan KR (2011) Numerical simulations of wave setup over barred beach  
941 profiles: implications for predictability. *Journal of Waterway, Port, Coastal, and Ocean*  
942 *Engineering*, doi:10.1061/(ASCE)WW.1943-5460.0000076.

943 Stockdon H F, Holman R A, Howd P A, Sallenger A H (2006) Empirical parameterization of  
944 setup, swash, and runup. *Coastal Engineering* 53:573-588, 10.1016/j.coastaleng.2005.12.005

945 Talke SA, Kemp AC, Woodruff J (2018) Relative Sea Level, Tides, and Extreme Water Levels  
946 in Boston Harbor From 1825 to 2018. *J Geophys Res* <https://doi.org/10.1029/2017JC013645>

947 Testut L, Wöppelmann G, Simon B, Téchiné P (2006) The sea level at Port-aux-Français,  
948 Kerguelen Island, from 1949 to the present. *Ocean Dynamics* 56: 464–472. 10.1007/s10236-  
949 005-0056-8

950 Tregoning P, Lambeck K, Ramillien G (2008) GRACE estimates of sea surface height  
951 anomalies in the Gulf of Carpentaria. *Australia Earth Planet. Sc. Lett.* 271:241-244

952 Vignudelli S, Benveniste J, Birol F, FuLL, Picot N (submitted) Satellite altimetry  
953 measurements of sea level in the coastal zone. *Surveys in Geophysics*.

954 Wahr J, Molenaar M, Bryan F (1998) Time-variability of the Earth's gravity field:  
955 Hydrological and oceanic effects and their possible detection using GRACE. *J. Geophys. Res.*  
956 103:32,205–30,229.

957 Watkins M M, Wiese D N, Yuan D-N, Boening C, Landerer F W (2015) Improved methods  
958 for observing Earth's time variable mass distribution with GRACE. *JGR Solid Earth* 120:2648–  
959 2671. 10.1002/2014JB011547.

960 Watson C, Coleman R, White N, et al (2003) Absolute Calibration of TOPEX/Poseidon and  
961 Jason-1 Using GPS Buoys in Bass Strait, Australia Special Issue: Jason-1  
962 Calibration/Validation. *Mar Geod* 26:285–304. doi: 10.1080/714044522

963 Watson C, Coleman R, Handsworth R (2008) Coastal Tide Gauge Calibration: A Case Study  
964 at Macquarie Island Using GPS Buoy Techniques. *J Coast Res* 1071–1079. doi: 10.2112/07-  
965 0844.1

966 Watts D R, Kontoyiannis H (1990) Deep-Ocean Bottom Pressure Measurement: Drift Removal  
967 and Performance *J. Atmos. Ocean. Tech.* 7:296–306, doi:10.1175/1520-0426

968 Weissman DE, Morey S, Bourassa M (2017) Studies of the effects of rain on the performance  
969 of the SMAP radiometer surface salinity estimates and applications to remote sensing of river  
970 plumes," *IEEE International Geoscience and Remote Sensing Symposium (IGARSS)*, Fort  
971 Worth, TX, 2017, pp. 1491-1494, doi: 10.1109/IGARSS.2017.8127250  
972

- 973 Wiese D N, Landerer F W, Watkins M M (2016) Quantifying and reducing leakage errors in  
974 the JPL RL05M GRACE mascon solution, *Water Resour. Res.*, 52, 7490–7502.
- 975 Willis, J K, Chambers D P, Nerem R S (2008) Assessing the Globally Averaged Sea Level  
976 Budget on Seasonal to Interannual Time Scales. *J. Geophys. Res.* 113:C06015.  
977 doi:10.1029/2007JC004517.
- 978 Woodworth PL, Blackman DL (2002) Changes in extreme high waters at Liverpool since 1768.  
979 *Int J Climatol* 22: 697–714. 10.1002/joc.761
- 980 Woodworth P L, Pugh DT, Bingley RM (2010) Long-term and recent changes in sea level in  
981 the Falkland Islands. *J Geophys Res* 115:C09025.10.1029/2010JC006113.
- 982 Woodworth PL, Gravelle M, Marcos M, Wöppelmann G, Hughes CW (2015) The status of  
983 measurement of the Mediterranean mean dynamic topography by geodetic techniques. *J Geod*  
984 89:811–827, DOI 10.1007/s00190-015-0817-1
- 985 Woodworth PL, Hunter JR, Marcos M, Caldwell P, Menendez M, I. Haigh (2017) Towards a  
986 global higher-frequency sea level dataset. *Geosci. Data J.* 3: 50–59, doi: 10.1002/gdj3.42
- 987 Woodworth PL, Melet A, Marcos M, Ray RD, Wöppelmann G, Sasaki YN, Cirano M, Hibbert  
988 A, Huthnance JM, Monserrat S, Merrifield MA (submitted) Forcing Factors Causing Sea Level  
989 Changes at the Coast. *Surveys in Geophysics*.
- 990 Wöppelmann G, Pouvreau N, Simon B (2006) Brest sea level record: a time series construction  
991 back to the early eighteenth century. *Ocean Dynamics* 56:487–497. 10.1007/s10236-005-0044-  
992 z
- 993 Wöppelmann G, Martín Míguez B, Bouin M-N, Altamimi Z (2007) Geocentric sea-level trend  
994 estimates from GPS analyses at relevant tide gauges world-wide. *Global Planet Change*  
995 57:396–406
- 996 Wöppelmann G, Marcos M, Coulomb A, Martín Míguez B, Bonnetain P, Boucher C, Gravelle  
997 M, Simon B, Tiphaneau P (2014) Rescue of the historical sea level record of Marseille (France)  
998 from 1885 to 1988 and its extension back to 1849–1851. *J Geod* 88:869–885. 10.1007/s00190-  
999 014-0728-6
- 1000 Wöppelmann G, Marcos M (2016) Vertical land motion as a key to understanding sea level  
1001 change and variability *Rev Geophys* 54.10.1002/2015RG000502.
- 1002 Wouters, B, Chambers D P (2010) Analysis of Seasonal Ocean Bottom Pressure Variability in  
1003 the Gulf of Thailand from GRACE. *Global and Planetary Change* 74.  
1004 doi:10.1016/j.gloplacha.2010.08.002.  
1005  
1006  
1007  
1008  
1009